universität wien

DIPLOMARBEIT

Titel der Diplomarbeit

„The pyrimidine nucleotide transporter Mrs12p mediates iron uptake into yeast mitochondria“

Melanie Rosalia Hassler

angestrebter akademischer Grad

Magistra der Naturwissenschaften (Mag. rer.nat.)

Wien, am 31.12. 2008

Studienkennzahl:	A 419
Studienrichtung:	Chemie
Betreuer:	O. Univ. - Prof. Dr. Rudolf Schweyen

Index

1 Abstract

Iron uptake into mitochondria is of key importance for iron-sulfur cluster biogenesis, for heme synthesis and for the function of many mitochondrial proteins. In *S. cerevisiae*, the mitochondrial carrier proteins Mrs3p and Mrs4p had previously been identified to be the main iron transporters under iron limiting conditions. However, several indications point to the possibility that these proteins do not represent the sole system of mitochondrial iron import. Interestingly, the mitochondrial pyrimidine nucleotide transporter Mrs12p had recently been found to function as multi-copy suppressor of the *mrs3/4*Δ phenotype and therefore is a possible candidate for low-affinity mitochondrial iron uptake.

In this work, Mrs12p's involvement in mitochondrial iron uptake and the role of pyridimine transport in the proteins's ability to suppress the *mrs3/4*Δ phenotype were studied.

FET3-expression in *mrs3/4/12*Δ and *mrs3/4*Δ mutants was monitored by GFP-expression and microarray data showing induction of genes belonging to the iron-regulon of a *mrs3/4/12*Δ mutant were compared to *mrs12*Δ gene expression. Both *FET3*-expression and genome wide expression profiling pointed to a role of Mrs12p in mitochondrial iron acquisition.

For studying the role of pyrimidine transport, a mutant in contact site II of Mrs12p was created. Overexpression of the mutated gene did not complement the *mrs12*Δ phenotype and no pyrimidine transport into mitochondria carrying the mutated protein was observed. Suppression of the *mrs3/4*Δ phenotype in growth tests was not seen and iron uptake into submitochondrial particles (SMPs) was significantly reduced when compared to wild-type SMPs or *mrs3/4*Δ SMPs overexpressing *MRS12*.

Besides suppression of the *mrs3/4*Δ phenotype, it had already been reported that overexpression of *MRS12* also suppresses the *mrs2*Δ phenotype, which is due to lack of mitochondrial Mg^{2+} uptake. Considering this, we assumed a function of Mrs12p in not only iron, but low-affinity divalent metal transport and therefore looked at mitochondrial Mg^{2+} uptake in more detail. Transport studies into mitochondria using the fluorescent Mg^{2+}-chelator mag-fura 2 showed that overexpression of *MRS12* enhances Mg^{2+} transport into *mrs2*Δ mitochondria, but no increase in Mg^{2+} transport was seen in the case of the mutant. Also, overexpression of the mutated gene did not suppress the *mrs2*Δ phenotype.

These observations imply that Mrs12p transports Fe^{2+} and Mg^{2+} into mitochondria together with pyrimidine nucleotides. The relevance of these results for divalent cation uptake into yeast mitochondria will be discussed in the last part of this work.

Zusammenfassung

Für Mitochondrien ist die Aufnahme von Eisen für die Eisen-Schwefel Cluster Biogenese, für die Haem-Synthese und für die Funktion vieler mitochondrialer Proteine von entscheidender Bedeutung. In *S. cerevisiae* hatte man bereits zwei mitochondriale Carrier Proteine, Mrs3p und Mrs4p, identifiziert, welche für den Eisentransport unter Eisenmangelzustand verantwortlich sind. Einige Beobachtungen weisen jedoch darauf hin, dass diese Proteine nicht das einzige System zur Eisenaufnahme ausmachen. Interessanterweise ist der mitochondriale Pyrimidin-Nukleotid Transporter Mrs12p in der Lage, als Multi-Copy Suppressor des *mrs3/4*Δ Phenotyps zu wirken und stellt daher einen Kandidaten für Eisenaufnahme bei normalen Eisenkonzentrationen in der Zelle dar.

In dieser Arbeit soll die Beteiligung von Mrs12p an der mitochondrialen Eisenaufnahme und die Rolle, die der Pyrimidintransport bei der Suppression des *mrs3/4*Δ Phenotyps spielt, untersucht werden.

Die Expression von *FET3* einer *mrs3/4/12*Δ und einer *mrs3/4*Δ Mutante wurde mittels GFP-Expression beobachtet und Microarray Daten, welche die Induktion von Genen des Eisen-Regulons einer *mrs3/4/12*Δ Mutante aufzeigen, wurden dargestellt und mit der Genexpression einer *mrs12*Δ Mutante verglichen. *FET3*-Expression und Expression Profiling weisen auf eine Rolle von Mrs12p beim mitochondrialen Eisen-Erwerb hin.

Um die Rolle des Pyrimidin-Transports zu untersuchen, wurde eine Mutante im Kontaktpunkt II von Mrs12p hergestellt. Überexpression des mutierten Gens führte zu keiner Suppression der *mrs12*Δ Mutante und keine Pyrimidin-Aufnahme konnte in Mitochondrien, welche das mutierte Protein besaßen, beobachtet werden. In Wachstumstests wurde keine Suppression des *mrs3/4*Δ Phenotyps gesehen und Eisen-Aufnahme in submitochondriale Partikel (SMPs) war im Vergleich zu Wild-Typ SMPs oder *mrs3/4*Δ SMPs, die *MRS12* überexprimierten, deutlich reduziert.

Vor dieser Arbeit war bereits bekannt, dass Überexpression von *MRS12*, außer zur Suppression des *mrs3/4*Δ Phenotyps, auch zur Suppression des *mrs2*Δ Phenotyps führt. Dieser Phenotyp kommt durch das Fehlen des mitochondrialen Mg^{2+} Transporters Mrs2p zustande. Das führte uns zu der Annahme, dass Mrs12p nicht nur eine Funktion als Eisentransporter, sondern als Transporter mit geringer Affinität zu verschiedenen divalenten Metallen haben könnte. Daher untersuchten wir die mitochondriale Mg^{2+}-Aufnahme im Detail mittels Transportstudien an Mitochondrien mit dem fluoreszierenden Mg^{2+}-Chelator mag-fura 2. Diese zeigten, dass Überexpression von *MRS12* den Mg^{2+} Transport fördert, bei Expression

der Mutante wurde jedoch keine Zunahme gesehen. Überexpression des mutierten Gens führte auch zu keiner Suppression des *mrs2*Δ Phenotyps.

Diese Beobachtungen zeigen, dass Fe^{2+} und Mg^{2+} gemeinsam mit Pyrimidin-Nukleotiden von Mrs12p in die Mitochondrien transportiert werden. Abschließend wird die Bedeutung dieser Ergebnisse für die Aufnahme divalenter Kationen in die Mitochondrien der Hefe diskutiert.

2 Introduction

2.1 The Role of Iron and its Acquisition by Living Cells

Iron is of key importance to the biology of all eukaryotes and the vast majority of prokaryotes. Its ability to shift between two redox states and to gain and lose electrons easily makes it a perfect candidate for the metal centers of nature's redox reaction performing enzymes. The metal is involved in vital biological processes like oxygen transport, oxidative phosphorylation, DNA biosynthesis, and xenobiotic metabolism (Hentze, Muckenthaler et al. 2004) and it is part of such important proteins as cytochromes, oxygenases, flavoproteins, and redoxins. In mammalian hemoglobin, it provides a specific binding site for oxygen and thereby enables oxygen delivery to tissues of multicellular organisms (Andrews 2000). Although iron belongs to the most abundant metals on earth, it is poorly bioavailable, as it is generally present in the ferric (Fe^{3+}) form, which is almost insoluble in water at neutral pH. A second problem of iron chemistry for organisms is that the metal's ability to donate electrons can lead to the formation of free radicals; when ferrous iron (Fe^{2+}) interacts with H_2O_2, it undergoes the Fenton reaction (Papanikolaou and Pantopoulos 2005). The Fenton reaction produces ferric iron, $^{\cdot}OH$, and the hydroxyl radical, whereby the latter may attack adjacent lipids and lead to oxidative damage of DNA and other macromolecules. For these reasons, complex iron-transport and management systems have evolved in virtually all organisms, which will be discussed in more detail below.

2.1.1 Iron Acquisition by Living Cells

Bacteria. In bacteria, when intracellular iron level is elevated, the protein Fur (for ferric uptake regulator) is expressed, whose function is to repress transcription initiation of iron-uptake genes (Ernst, Bennett et al. 1978). When growing under iron depletion conditions, bacteria produce low-molecular-weight molecules called siderophores. The siderophores are secreted into the environment and make iron soluble before it is transported inside the cell. The iron-siderophore complex binds to outer-membrane receptors and is actively transported across the outer and the inner membrane into the cytoplasm. Here, it is assumed that the metal is released from the siderophore, reduced to the soluble ferrous iron (Fe^{2+}), and sequestered into iron-using proteins (Masse and Arguin 2005).

Yeast. In *S. cerevisiae*, there are several transport systems that transfer iron across the cell surface (Van Ho, Ward et al. 2002). Two non-specific or low-affinity transport systems are located at the plasma membrane. These proteins, which are products of the *FET4* and *SMF1* genes, not only transport iron, but can also take up other transition metals. In addition to these low-affinity systems, there are two high- affinity transport systems, providing the cell with the

ability to adjust its uptake system under iron-deplete conditions. The first system involves the transport of siderophore-iron complexes, similar to those of bacteria, whereas the second transport system is comprised of two cell surface proteins, Fet3p, a multicopper oxidase, and Ftr1p, a transmembrane permease. Fet3p oxidizes ferrous iron to ferric iron and Ftr1p transports ferric iron across the plasma membrane (Kaplan, McVey Ward et al. 2006). The cell surface metalloreductases Fre1p and Fre2p provide the substrate for Fet3p by reducing Fe^{3+} and passing on Fe^{2+} to Fet3p (Georgatsou and Alexandraki 1994). Increased expression of iron transport genes is induced by the activity of the iron-sensing transcription factor Aft1p (Yamaguchi-Iwai, Dancis et al. 1995) and its paralogue Aft2p, which is able to bind to the promoter elements of genes that code for cell surface iron transporters (Rutherford, Jaron et al. 2003). When cells suffer from low iron, Aft1p relocalizes to the nucleus. There, it functions as an activating transcription factor for the promoters on approximately 20 genes, usually referred to as the iron-regulon (Yamaguchi-Iwai, Ueta et al. 2002; Shakoury-Elizeh, Tiedeman et al. 2004, **Figure 1**). Induction of these genes increases the cell's ability for iron uptake and remodels intracellular metal homeostasis in response to low iron levels.

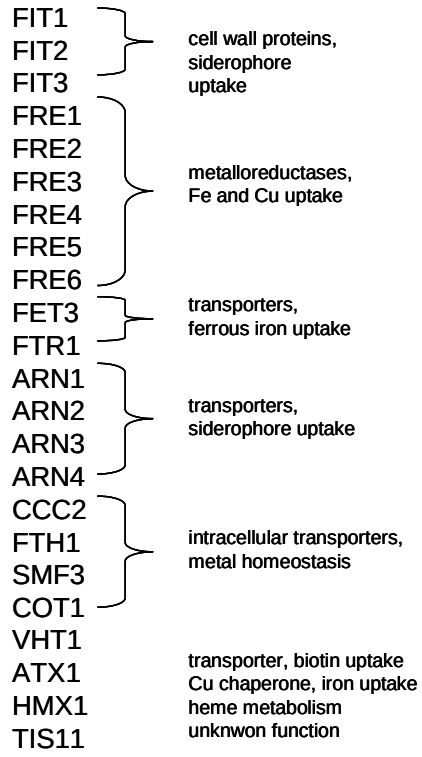

Figure 1: The Iron Regulon of *S. cerevisiae*. The iron-regulon comprises cell wall proteins involved in siderophore uptake (*FIT1*, *FIT2*, *FIT3*), metalloreductases for iron and copper uptake (*FRE1*, *FRE2*, *FRE3*, *FRE4*, *FRE5*, *FRE6*), transporters for ferrous iron uptake (*FET3*, *FTR1*) and siderophore uptake (*ARN1*, *ARN2*, *ARN3*, *ARN4*), intracellular transporters which play a role in metal homeostasis (*CCC2*, *FTH1*, *SMF3*, *COT1*) and proteins of biotin uptake, copper or heme metabolism or of unknown function (*VHT1*, *ATX1*, *HMX1*, *TIS11*).

Mammals. In mammals, iron is absorbed from the diet in the duodenal part of the intestines by the divalent metal transporter 1 (DMT1, also called Nramp2 and DCT1 (Gunshin, Mackenzie et al. 1997)). Export of iron (as Fe^{2+}) from the barrier cells of the duodenum and release into the blood is mediated by ferroportin (also referred to as IREG1 and MTP1 (McKie, Marciani et al. 2000)). Ferroportin either cooperates with hephaestin (Vulpe, Kuo et al. 1999) or ceruloplasmin (Harris, Durley et al. 1999), multicopper oxidases that convert Fe^{2+} into Fe^{3+} (ceruloplasmin is a homologue of yeast Fet3p). As iron is able to bind to many proteins, it is transported in the serum in the Fe^{3+} form by a specific carrier, transferrin (Ponka, Beaumont et al. 1998), which also ensures that iron stays in the non-reactive ferric form and does not engage in electron transfer reactions. When cells need iron, they take up transferrin that contains bound iron by transferrin receptors. These proteins are present on the cell surface in amounts depending on the cell's demand for iron. The transferrin-transferrin receptor-complex is internalized by clathrin-mediated endocytosis. Endosomes are acidified by vesicular membrane proteins that pump protons, and iron is released from transferrin upon the change in pH. Apotransferrin and the transferrin-receptor are recycled back to the plasma membrane, where apotransferrin dissociates from the receptor upon normal pH (Hentze, Muckenthaler et al. 2004). The iron in the acidified endosome is transferred via DMT1 to the cytoplasm, where it is either used for cellular proteins and processes requiring iron or stored by the major iron-storage protein ferritin (Harrison and Arosio 1996) (**Figure 2**).

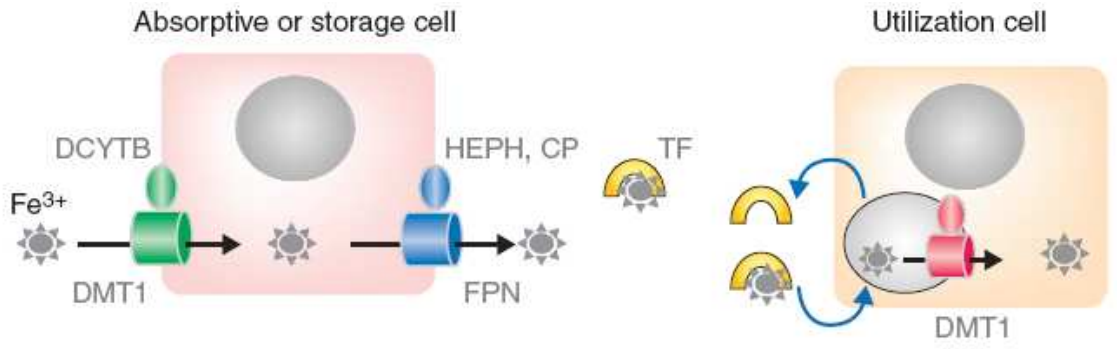

Figure 2: Iron Distribution and Storage inside Mammalian Cells. Iron (III) from the diet is reduced by DCYTB (duodenal cytochrome *b*-like ferrireductase) and iron (II) enters absorptive cells of the intestinal epithelium or storage cells through DMT1 (divalent metal transporter 1). Export of iron (III) is mediated by ferroportin (FPN) after oxidation of iron (II) by hephaestin (HEPH) or ceruloplasmin (CP). In the serum, iron (III) is transported by transferrin (TF) and the TF-iron (III) complex is taken up by transferrin receptors into endosomes of cells needing iron. The iron in the endosome is transferred via DMT1 to the cytoplasma, where it is used for proteins or stored by ferritin (Andrews 2002).

Regulation of iron acquisition by the cell is mediated via several pathways. The mRNA of the transferrin receptor, for example, contains iron-regulatory elements (IREs) (Casey, Hentze et al. 1988), which are recognized by iron-regulatory proteins (IRPs) (Hentze and Kuhn 1996). IRPs are activated under iron-deplete conditions and promote translation of transferrin receptor mRNA. The transferrin receptor is further regulated at the transcriptional level by dimerized hypoxia inducible factor (HIF-1α and HIF-1β) (Lok and Ponka 1999), which enhance promoter activity, and at protein level by the hereditary hemochromatosis protein (HFE), which binds to the transferrin receptor in competition with transferrin and so blocks transferrin binding (Lebron, West et al. 1999). A negative regulator of plasma iron is hepcidin, a peptide hormone which inhibits iron efflux by binding ferroportin and leading to the degradation of the iron exporter (Nemeth, Tuttle et al. 2004). Thus, regulation of iron metabolism in mammals occurs mainly by controlling the rate of iron absorption by the body, as there is no known mechanism for up-regulation of iron excretion.

2.2 Iron Linked Disorders

A reason to gain more insight into the molecular mechanisms of iron metabolism is that there are several iron linked disorders which affect humans. Two main types of disorders can be distinguished: iron-overload and iron-deficiency disorders. The latter consist of genetic and acquired anaemias. In hereditary anemias, specific transporters or auxiliary proteins which are involved in iron acquisition are absent or show reduced function and thereby lead to reduced iron levels in the body. Acquired anaemias are usually the result of inflammatory reactions mediated by the immune system to fight bacterial infections, as limited access to iron slows down bacterial growth (Schaible and Kaufmann 2004). In iron-overload disease, the binding capacity of transferrin is exceeded by plasma iron levels. The body is not able to downregulate iron absorption in response to increased iron stores and the elevated iron levels cause tissue damage and fibrosis. Primary iron-overload disease or hereditary haemochromatosis (HH) is the result of a genetic misregulation of iron acquisition. So far, HH has been linked to defects in four genes, three of these defective genes are involved in inadequate hepcidin production and the forth is caused by mutations in the iron exporter ferroportin (De Domenico, McVey Ward et al. 2008).

As iron transport and iron homeostasis in mitochondria will be addressed in this work, it is also of interest to mention the disease Friedreich ataxia, a cardiac and neurodegenerative disorder. Here, iron accumulation in mitochondria is seen in the heart and central nervous system of affected patients due to decreased levels of the frataxin transcript. The frataxin

protein is proposed to participate in Fe-S cluster biogenesis (Pandolfo 2008), but the exact mechanism of its function is still unclear.

2.3 Iron Homeostasis in Mitochondria

Before addressing iron transport into mitochondria, I'd like to give a general overview on mitochondria and iron homeostasis. Mitochondria form an essential part of the cell volume of eukaryotic cells and have been crucial for the evolution of complex animals. The most significant role of the organelle is the generation of ATP through oxidation of pyruvate by O_2 to CO_2 and H_2O, which leads to a 15 times increased ATP production than that by glycolysis alone. Also, other key metabolic processes like fatty acid oxidation or iron-sulfur cluster biogenesis are localized inside the mitochondrial matrix. The mitochondrion is enclosed by a double membrane; the volume between the outer and the inner membrane is called the intermembrane space. The outer membrane is permeable to all molecules of 5000 daltons or less, whereas the highly convoluted inner membrane contains specific transport proteins for selective substrate uptake and is impermeable to ions (Alberts, Johnson et al. 2007).

However, ions, especially iron, play an important part in the function of many mitochondrial proteins or metabolites. Iron is required for the generation of hemoproteins, for iron-sulfur cluster (Fe-S) containing proteins of the matrix (e.g. aconitase, biotin synthase, homoaconitase and ferredoxin) and the inner membrane and as cofactor in a class of enzymes which contain oxo-bridged binuclear iron centers (Pierrel, Cobine et al. 2007). Recent studies in *S. cerevisiae* show that mitochondrial iron homeostasis is regulated by components of the Fe-S cluster biogenesis system, as yeast strains that were depleted of Fe-S cluster scaffold proteins, chaperone proteins or ferredoxin involved in Fe-S cluster assembly accumulated iron in their mitochondria (Knight, Sepuri et al. 1998; Li, Kogan et al. 1999; Schilke, Voisine et al. 1999) and thereby demonstrating that Fe-S clusters are crucial for maintaining mitochondrial iron homeostasis. Mutations in these proteins lead to activation of the iron-sensing transcription factor Aft1p in *S. cerevisiae* (described above) and increased cellular iron-uptake (Li, Kogan et al. 1999).

2.3.1 The Mitochondrial Carrier Proteins Mrs3/4p and Iron Transport

Regarding the important role of iron in mitochondrial metabolism and Fe-S cluster biogenesis, the question of its import into mitochondria has been of keen interest. The first mechanistic studies of iron import into yeast mitochondria showed that iron uptake is driven energetically by a membrane potential across the inner membrane, but does not require ATP (Lange, Kispal et al. 1999). In *S. cerevisiae*, the two inner membrane proteins Mrs3/4p could be linked to

mitochondrial iron acquisition (Muhlenhoff, Stadler et al. 2003). *MRS3* and *MRS4* genes had initially been identified in a screen for multicopy suppressors of a mitochondrial RNA splicing defect (Wiesenberger, Link et al. 1991) and suppressed the phenotype caused by the absence of the mitochondrial Mg^{2+} transporter Mrs2p (Waldherr, Ragnini et al. 1993). The two proteins show high sequence similarity and belong to the mitochondrial carrier family, a family of carriers found in the inner mitochondrial membrane of eukaryotes. Proteins of this family contain six membrane-spanning segments and have a tripartite structure. Their substrates vary from protons transported by the uncoupling protein up to large molecules such as ATP and ADP exchanged by the ADP/ATP carrier (Palmieri, Agrimi et al. 2006). A hint towards *MRS4* function came from genome-wide transcription profiling of an *AFT2-1*^{up} mutant, indicating that the gene is co-induced with several iron uptake genes and suggesting a role of this carrier in mitochondrial metal transport (Rutherford, Jaron et al. 2001). Further experiments showed that deletion of *MRS3/4* in a frataxin deletion mutant (Δ*yfh1* cells) is able to suppress mitochondrial iron accumulation, that overexpression of *MRS4* in Δ*yfh1* cells leads to higher mitochondrial iron content and that overexpression of *MRS4* in wild-type cells results in increased heme formation (Foury and Roganti 2002). Cells deleted in *MRS3/4* show increased vacuolar iron transport and decreased cytosolic iron, demonstrating that expression levels of mitochondrial proteins can not only alter mitochondrial, but also cellular and vacuolar iron homeostasis (Li and Kaplan 2004). In the publication of Mühlenhoff *et al*., genome-wide expression profiling of strains deleted in *MRS3/4* lead to up-regulation of several genes of the "iron regulon", indicating that the two proteins participate in cellular iron metabolism. Biochemical studies *in vivo*, *in organello* and *in vitro* revealed that altered heme formation activities in *mrs3/4*Δ cells and cells overexpressing *MRS3/4* were caused by alterations of mitochondrial iron uptake. However, this observation only became evident under iron-deplete conditions, as no influence of *MRS3/4* expression levels on iron utilization in mitochondria isolated from cells grown in iron-replete medium could be detected. In iron-replete medium, enough iron was able to enter the mitochondrion, even in absence of Mrs3/4p. Recent transport studies using submitochondrial particles (SMPs) showed that iron does not enter *mrs3/4*Δ SMPs, whereas it is readily taken up into SMPs prepared from wild-type cells (Froschauer, unpublished results).

The observations by Mühlenhoff *et al*. imply that there are other ways for iron to be transported into the mitochondria, provided that the iron concentration in the cytosol is sufficient. To discover novel proteins involved in yeast mitochondrial iron import, our group performed a multi-copy suppressor screen. In this screen, a *mrs3/4*Δ strain was transformed

with a wild-type yeast genomic library and transformants were screened on media containing low iron concentrations to detect genes which were able to suppress the *mrs3/4*Δ growth defect on low iron. The gene which was found with maximum frequency under the conditions of the screen was *MRS12/RIM2* (Wiesenberger, Binder, unpublished data).

2.3.2 The Mitochondrial Pyrimidine Carrier Mrs12p/Rim2p

MRS12/RIM2 has originally been identified as a multicopy suppressor of the *mrs2*Δ phenotype, which results from absence of the main mitochondrial Mg^{2+} transporter Mrs2p (Van Dyck, Jank et al. 1995). It is, like *MRS3/4*, a member of the mitochondrial carrier family and has been shown to transport (deoxy)pyrimidine nucleoside triphosphates into mitochondria in exchange for (deoxy)pyrimidine nucleoside monophosphates (Marobbio, Di Noia et al. 2006). Cells deficient in *MRS12/RIM2* lose their mitochondrial DNA and show, compared to wild-type ρ^0 cells, a slow-growth phenotype on media containing glucose (Van Dyck, Jank et al. 1995).

2. 4 The Topic of this Work

To date, there was no known connection between mitochondrial iron uptake and Mrs12p/Rim2p function. However, in our search for a low-affinity mitochondrial iron transporter mediating uptake under iron replete-conditions we identified *MRS12/RIM2* (further referred to as *MRS12*) as multi-copy suppressor of the high-affinity iron transporters *MRS3/4*. This finding prompted us to take a closer look on Mrs12p/Rim2p (further referred to as Mrs12p) function and to characterize it in relation to mitochondrial iron homeostasis.

Therefore, the first task of this work consisted in examining if there was a relation between *MRS12* expression and cellular iron homeostasis. In order to investigate this, a *FET3*-GFP assay and subsequent genome wide expression profiling were performed. To test the involvement of pyrimidine transport in iron import mediated by Mrs12p, a mutant defective in pyrimidine transport was created and analysed in suppression studies and SMP experiments. The second task was to see if Mrs12p is also able to mediate mitochondrial Mg^{2+} uptake, as suppression of the *mrs2*Δ phenotype by *MRS12* had been described before. Here, the mutant was compared to wild-type Mrs12p in mitochondrial Mg^{2+} uptake studies using the Mg^{2+} chelator mag-fura 2 and in growth tests.

3 Materials and Methods

3.1 Yeast Strains and Media

All yeast strains used in this work are listed in the following table.

Name	Background	Genotype	Notes
W303-1A		*MATa, ura3–1, ade2–1, trp1–1, his3–11,15, leu2–3,112*	ATCC no. 208353
DBY747		*MATa, his3-Δ1, leu2-3, leu2-112, ura3-52, trp1-289a*	ATCC no. 204659
W303 ρ^0	W303-1A	no mitochondrial DNA	by Dr. G. Wiesenberger
DBY747 ρ^0	DBY747	no mitochondrial DNA	by Dr. G. Wiesenberger
GW400	W303-1A	*mrs3Δ::loxP; mrs4Δ::loxP*	by Dr. G. Wiesenberger
GW400 ρ^0	W303-1A	*mrs3Δ::loxP; mrs4Δ::loxP,* no mitochondrial DNA	by Dr. G. Wiesenberger
GW403	DBY747	*mrs3Δ::loxP; mrs4Δ::loxP*	by Dr. G. Wiesenberger
GW403 ρ^0	DBY747	*mrs3Δ::loxP; mrs4Δ::loxP,* no mitochondrial DNA	by Dr. G. Wiesenberger
OS1-3c	W303-1A	*mrs12::kanMX4*	by Dr. G. Wiesenberger
OS1-2d	W303-1A	*mrs3Δ::leu2; mrs4Δ::ura3; mrs12::kanMX4*	by Dr. G. Wiesenberger
YAS1	W303-1A	*MRS12/mrs12::kanMX4*	by Axel Struß
JJ1A		*MATa, arg1, thr1*	Laboratory Stock
JJ1C		*Matα, arg1, thr1*	Laboratory Stock

Table 1: Yeast Strains.

The composition of media and buffers was as follows:

Name	Composition
LB Amp	1% tryptone, 0.5% yeast extract, 1% NaCl, 0.1% glucose, 2% agar, 0.02% ampicillin
YPD	2% peptone, 1% yeast extract, 2% glucose, (2% agar for plates)
2×YPAD	4% peptone, 2% yeast extract, 4% glucose, 0.4% adenine
YPG	2% peptone, 1% yeast extract, 3% glycerine, (2% agar for plates)
SD complete	0.67% yeast nitrogen base, 2% glucose, 2% agar, amino acids and supplements as required
SD w/o	0.67% yeast nitrogen base, 2% glucose, 2% agar
Cadmium plates	YPD supplemented with 10, 20,30, 40 and 60 μM Cd^{2+}
BPS plates (low iron)	YPD with 100 μM BPS (bathophenanthrolinedisulfonate, Sigma),supplemented with 0, 1, 2 and 3 μM Fe^{2+} (5 μM $FeCl_2 \cdot 4H_2O$, 5 μM β-mercaptoethanol, 0.1 M HCl)
sporulation plates	1% potassium-acetate, 0.1% yeast extract, 0.025% glucose, 2% agar
G418 plates	YPD with 200 μg/ml geneticin
buffer I	10 mM Tris·SO_4 (pH 9.4), 10 mM DTT is added prior before use
buffer II	1.2 M Sorbitol, 20 mM KPi pH 7.4
buffer III	0.6 M sorbitol, 20 mM Tris·HCl pH7.4
sucrose buffer	250 mM sucrose, 10 mM Tris·HCl pH 7.4
TES	100 mM Tris·HCl, 100 mM EDTA, 2% SDS
1*SSC	3 M NaCl, 0.3 M Na_3citrate·$2H_2O$, pH 7.0
20×TAE buffer	9.68% Tris base, 2.38% glacial acid acid, 0.02 M EDTA (pH 8.0)
30% acrylamide mix	30 % acrylamide, 0.8 % bisacrylamid
4×loading dye	200 mM Tris·HCl (pH 6.8), 400 mM dithiothreitol, 8% SDS, 0.4% bromophenol blue, 40% glycerol
5×running buffer	15 g Tris, 72 g glycine, 50 ml 10% SDS
staining solution	40% methanol, 7% acetic acid, 0.025% Coomassie Brilliant Blue G250
destaining solution	20% methanol, 7.5% acetic acid
transfer buffer	5.8 g Tris·HCl, 2.9 g glycine, 0.37 g SDS, 200 ml methanol, pH 8.3
TBS-T	0.88% of NaCl, 0.02% of KCl, 0.3% Tris base (pH 7.4), 1% Tween-20

Table 2: Media and Buffer Composition.

3.2 Gene Expression Profiling

3.2.1 Growing of Cells

Wild-type (W303 ρ^0) and isogenic mutant strain (*mrs3*Δ, *mrs4*Δ, *mrs12*Δ) were grown overnight in SD complete medium to an OD_{600} of about 1, diluted to an OD_{600} of 0.3 in SD complete, grown to an OD_{600} of 1.5 and harvested. Cell pellets were washed, frozen in liquid nitrogen and stored at -80°C.

3.2.2 RNA Isolation

The pellet was resuspended in TES solution, equal amounts of acid phenol were added, the solution was vortexed and incubated 45 minutes at 65°C with vortexing every 10 minutes. The pellet was placed on ice for 5 minutes, microcentrifuged at 15 000 rpm for 5 minutes at 4°C. This extraction step was repeated once. Then, the aqueous top phase was transferred to a new tube, chloroform was added, the tube was vortexed and then centrifuged at 15 000 rpm for 5 minutes, 4°C. Again, the aqueous phase was transferred to a new tube, 1/10 of solution

volume of 3M sodium acetate, pH 5.3, and 2.5 times solution volume of ice-cold 100% ethanol were added and the solution was put at -80°C for one hour. Then, the tube was centrifuged for 10 minutes, 15 000 rpm, 4°C and 1 ml of ice-cold 70% ethanol was added. The tube was centrifuged for 5 minutes at 15 000 rpm, 4°C and the supernatant was taken off, this step was repeated. The tube was left open at RT for 5 minutes, then the pellet was solved in 35-40 µl of DEPC-H_2O and the solution was put at 65°C for 10 minutes. 1 µl of the well solved RNA was pipetted to 750 µl of water, the concentration was determined by measuring OD_{260} (ε_{RNA} = 40 $L \cdot mol^{-1} \cdot cm^{-1}$).

3.1.3 cDNA Generation

30 µg of total RNA were dissolved in RNAse free water, anchored oligo-dT primer (5'-TTT TTT TTT TTT TTT TTT TTV N-3', MedProbe) was added and the solution was incubated at 65°C for 10 minutes. For each of the two labeling reactions, a reaction mix containing 5×first strand buffer (Invitrogen), 0.1M DTT (Invitrogen), dNTP (dATP, dCTP and dGTP 20 mM, dTTP 8 mM, Amersham), Cy3-dUTP or Cy5-dUTP (Amersham) and Superscript II (200 U/µl, Invitrogen) were made and the annealed primer and RNA were added to the mixture. The solution was incubated at 42°C for 25 minutes, then 1 µl of enzyme was added as reaction booster and the mixture was incubated for another 35 minutes at 42°C. To stop the RT-reaction, 0.1M NaOH/2 mM EDTA was added and the solution was incubated at 65°C for another 15 minutes. Equal amounts of 0.1M HCl were added to neutralize the solution and cDNA purification was carried out using the CyScribe GFX Purification Kit (GE Healthcare). Wild-type Cy3 and mutant Cy5 elution solutions or verse visa were combined. Then, the sample volume was reduced to 5 µl or less by the use of a Speed-Vac (Hetovac, VR-1).

3.1.4 Hybridization, Washing and Scanning

To each 100 µl of DIG Easy Hyb solution (Roche) 10 µl of ssDNA (10 mg/ml) were added and the mixture was incubated at 65°C for two minutes. 80 µl of the prepared hybridization solution were added to the pooled pair of Cy5 and Cy3-labelled cDNA and incubated at 65°C for two minutes. The mixture was carefully pipetted onto the microarrays carrying coverslips, the microarrays were placed into a hybridization chamber partly filled with DIG Easy Hyb solution, the chamber was wrapped with plastic wrap and put into a box lined with wet towel papers. The box was placed at 37°C overnight for hybridization. The next day, the coverslip was removed by dipping the array in 1×SSC and the arrays were washed three times for 15 minutes at 50°C in 50 ml Greiner tubes containing pre-warmed 1×SSC/0.1% SDS. The slides were rinsed twice at RT 1× SSC and then in 0.1×SSC and dried by centrifugation at 500 rpm

for 5 minutes. Arrays were stored in the dark, scanned with GenePix Pro 4.1 and further analyzed using the program limma (Linear Models for Microarray Data).

3.2 FET3-*GFP Assay*

Yeast strain W303 ρ^0 and isogenic mutant strains (*mrs3/4*Δ, *mrs12*Δ, *mrs3/4/12*Δ) were transformed with a plasmid containing the *FET3*-GFP fusion protein with -trp as marker. Colonies emerging on –trp plate were picked and grown on patches on –trp plates overnight. Cells were checked for fluorescence under the fluorescence microscope (Zeiss, Axioplan 2). Cells containing the *FET3*-GFP fusion protein were grown in –trp medium with ferric ammonium citrate (0.5 g/10 ml stock, diluted 1:1000) overnight, diluted to an OD_{600} of 0.15 in –trp medium containing ferric ammonium citrate and grown to an OD_{600} of 0.5. Cells without plasmid were used as controls. The cells were harvested by centrifugation (3 ml OD_{600} of 1, 4500 rpm, 4 min) and resuspended in 3 ml of water. The fluorescence was determined using the Perkin Elmer LS55 spectrofluorometer (FFA). The excitation wavelength was set at 480 nm and the emission wavelength was recorded from 505 to 550 nm. GFP emission maximum was measured at 510 nm. All measurements were performed at 25°C in 3 ml cuvetts containing 2 ml solution under stirring conditions.

3.3 Construction of mrs12 *G245Y S246A by* In Vitro *Mutagenesis*

3.3.1 Primer Construction

The gene sequence of *MRS12* was obtained from the *Saccharomyces* Genome Database (http://www.yeastgenome.org) and contact point II which was to be changed was identified. To mutate the amino acids glycine (gene sequence GGT) and serine (gene sequence TCT) at contact point II into tyrosine (gene sequence TAT) and alanine (gene sequence GCT), two primers containing these sequences were constructed. For easy identification of the desired mutation, an EcoRI restriction site was introduced close to the mutation by changing the AccI restriction site GTATAC to GAATTC (EcoRI restriction site).

mrs12mGSfw :
5’-TTGAGTGCCTCTTATTTGTATGCTGTTGAAGGAATTCTTCAATGGCTATTATATG-3’
mrs12mGSrv :
5’-ATATAATAGCCATTGAAGAATTCCTTCAACAGCATACAAATAAGAGGCACTCAAC-3’

Outside primers were placed in the polylinker region of the template plasmid.

pCM189fw :
5'-AAATTACCGGATCAATTCG-3'
pCM189rv :
5'-CATAACTAATTACATGATGC-3'

The template plasmid contained the *MRS12* gene with an HA-tag (pAS14 in pCM189 background, see Appendix for plasmid maps). Plasmid maps were constructed using the program Clone Manager (Version 4.0).

3.3.2 PCR and DNA Gel Extraction

The two PCR mixes consisted of buffer DyNAzyme, $MgCl_2$ (final concentration 2.5 mM), dNTPs (0.2 mM), DyNAzyme-polymerase (proofreading, 1U/µl, Finnzymes), 0.5 µl plasmid DNA (pAS14 1 :10 dilution) as template and of primers pCM189fw and mrs12mGSrv (1 µM) or primers pCM189rv and mrs12mGSfw (1 µM) (50 µl total). The PCR was run for 30 cycles with an annealing temperature of 47°C and an extension time of 45 seconds. The PCR products were loaded onto a preparative gel (0.8% agarose, TAE buffer) and the bands were cut under UV light. The DNA was extracted from the gel with QIAquick gel extraction kit (Qiagen) according to protocol and eluted in elution buffer. The eluted PCR products were used as templates for the second PCR. This PCR was contained the same reagents like the first PCR, but here primer pCM189fw (1 µM), primer pCM189rv, 2.5 µl PCR product 1 and 2.5 µl PCR product 2 as templates were used (50 µl total). The PCR was run for 35 cycles with an annealing temperature of 47°C.

3.3.3 Restriction Digestion, Ligation and *E.coli* Transformation

To obtain the insert for cloning, the PCR product (containing *mrs12* G245Y, S246A) was cut with restriction enzyme BamHI (eight preparations were set up to increase the yield). The restriction digestions were pooled, loaded onto a preparative gel (0.8% agarose, TAE) and the DNA band at 1200 bp was cut under UV. The DNA was extracted with QIAquick gel extraction kit according to protocol and eluted in elution buffer.
The vector for insertion (here pAS14) was also cut with BamHI, 15 minutes before the end of the restriction digestion 1 µl of phosphatase was added for dephosphorylation of vector ends. The solution was heated at 75°C for 15 min to denature the phosphatase, loaded onto a

preparative gel, the band at 8300 bp was cut under UV light and the DNA was purified with QIAquick gel extraction kit as described above.

For the ligation, 50 ng of the cut and dephosphorylated vector, 20 ng of the cut insert, 1 µl of T4-ligase (Fermentas) and 1 µl 10×ligase buffer were filled up with sterile water to 10 µl and incubated at 16°C overnight. Controls without insert (religated vector) and without ligase (uncut vector) were also set up.

Competent *E.colis* DH10B ($CaCl_2$ Method, (Hanahan 1983)) were transformed with 5 µl of the ligation mix and plated onto LB Amp. For analysis, grown colonies were each inoculated into LB Amp medium and grown overnight.

3.3.4 Miniprep, Restricton Digestion and Sequencing

To obtain the plasmids, a miniprep was performed (Invisorb Miniprep kit, according to protocol). To check if the plasmid contained the desired *mrs12* G245Y S246A mutation, the DNA was cut with EcoRI. The plasmids containing the mutation were sent for sequencing and the sequences were checked by a BLAST search and with the programmes Chromas (Version 2.13) and Clustal (http://www.clustal.org). The plasmid with the *mrs12* G245Y S246A mutation in contact point II of *MRS12* and a C-terminal HA-tag was named pMH1.

3.3.5 Subcloning

To obtain the *MRS12* gene without the HA-tag, plasmid pMH1 was cut with NotI to get rid of the HA-tag. The isolation of the cut plasmid by gel extraction, the religation, the transformation and the identification by mini prep and restriction digestion (here with BamHI and PstI) were performed as described above. The resulting plasmid containing the *mrs12* G245Y S246A gene was called pMH2.

In a further step, the *MRS12* gene from plasmid pAS12 (*MRS12* in pCM189 backbone), the *mrs12* G245Y S246A gene from plasmid pMH2 and the *mrs12* G245Y, S246A gene with the HA-tag from plasmid pMH1 were cloned into the single-copy plasmid pOLU2, which contains the *MRS12* gene under its endogenous promoter (YCplac33 backbone). pOLU2 was cut with HindIII, phosphatase was added to dephosphorylate the vector, the DNA was loaded onto a preparative gel and the 6720 bp fragment (containing the backbone and the endogenous promotor) was isolated. pMH1, pMH2 and pAS12 were also cut with HindIII and added onto a gel. The DNA fragments containing the *mrs12* G245Y S246A part were isolated, the fragments were ligated to the vector backbone and the ligation transformed into competent *E.coli* as described above. Restriction digestions of the minipreps of the transformed *E.coli* cultures were performed with PstI and BamHI (vectors with desired pAS12 or pMH2

fragments) or BamHI only (vector with pMH1 fragment) to check the correct insertion and orientation of the fragments. The resulting plasmid with the wild-type *MRS12* gene from pAS12 was called pMH3, the plasmid with *mrs12* G245Y S246A -HA from pMH1 was called pMH4 and with *mrs12* G245Y S246A from pMH2 pMH5 (all YCplac33 backbone).

3.4 Tetrad Dissection

3.4.1 Yeast Transformation

The diploid strain YAS1 (W303-1A background, *MRS12*/*mrs12*Δ) was inoculated into 2×YPAD and grown overnight at 28°C. The cell titer was determined by measuring OD_{600}. The culture was diluted to an OD_{600} of 0.5 and incubated at 28°C for 3-4 hours to an OD_{600} of about 2 (two divisions). The cells were harvested by centrifugation (4500 rpm, 4 minutes) and washed in sterile water. The supernatant was removed and the cells were resuspended in the appropriate amount of 100 mM LiAc (ml 100 mM LiAc = portions = $0.1 \times OD_{600} \times$culture-volume). Portions of 1 ml were transferred to eppendorf tubes and the suspension was incubated at 30°C for 10 minutes. A microcentrifuge tube of carrier DNA (2 mg/ml) was prepared by denaturing in a boiling water bath for 10 minutes and chilling immediately on ice. The cell suspension was centrifuged at 7000 rpm for 1 minute and the supernatant was removed. The transformation mix containing 240 µl PEG (50% w/v), 36 µl 1M LiAc, 52 µl carrier DNA and 32 µl water with plasmid DNA (2-3 µl plasmid DNA was used) per sample was added to each pellet and the cells were resuspended by pipetting. The suspension was incubated at 30°C for 30 minutes, heat shocked at 42°C for 20 minutes and centrifuged at 7000 rpm for 1 minute. The transformation mix was removed, 150 µl of sterile water were pipetted onto the pellet and the suspension incubated for 5 minutes at RT. The cells were resuspended by pipetting or vortexing vigorously and then the cell solution was pipetted onto SD drop-out plates. The plates were incubated at 28°C for 2-4 days.

3.4.2 Sporulation, Tetrad Dissection and Analysis

Single colonies of the diploid strain YAS1 with the plasmids for complementation (here pMH3 and pMH5) and for the control (here YCpLac33) were streaked out on YPD plates as patches and grown overnight. The patches were transferred to sporulation plates and incubated 5 days at RT. 50 µl zymolyase-20TT (1.5 mg/ml in 1M sorbitol) was added to a small amount of cells (1.5 mg/ml in 1M sorbitol), vortexed and incubated 20 minutes at RT. 500 µl of sterile water were added and the solution was streaked out on a YPD plate. Spores were dissected by the use of a micromanipulator (Singer Instruments). Colonies were grown for two to three days and then analysed by replica-plating on YPD, the drop-out plate, G418

(geneticin, 200 µg/ml) and on SD w/o plates containing a lawn of either JJ1A (mating type a) or JJ1c (mating type α) cells.

3.5 Serial Dilutions

3.5.1 Serial Dilutions

The transformed strains to be tested for suppression were inoculated in 4 ml drop-out medium and grown overnight. Cultures were diluted to an OD of 1 and transferred to the first column of a microtiter plate and further diluted (first column: pure culture OD 1, then 1:10, 1:100 and 1:1000 dilutions). Cultures were transferred onto plates for analysing the phenotype. After transferring the solutions to all plates (YPD, YPG, Cadmium-plates, plates with low iron concentration), they were incubated at 28°C or 37°C for two to four days and then scanned.

3.6 Isolation of Yeast Mitochondria (Mitoprep)

Precultures were grown overnight in 5 ml YPD, then transferred to 200 ml and then to 1 l fresh YPD or in 5 ml and 200 ml SD medium and afterwards in 1 l YPD. Cells were harvested at 3500 rpm (Sorvall Instruments, GSA rotor, 5 minutes, RT) and resuspended in buffer I. The cells were grown at 37°C on the shaker for 15 minutes, centrifuged (3500 rpm, GSA, 5 minutes, RT) and the pellet resuspended in buffer II. After centrifugation, the pellet was weighed and resuspended in buffer II. 2 mg of zymolyase (in buffer II) per gram cells were added to the cell suspension and the suspension was incubated for 45 minutes at 28°C on the shaker. From now on, cells were kept on ice and the centrifuge and buffers were cooled. The cells were centrifuged (3500 rpm, 5 minutes, 4°C) and washed in buffer 2, centrifuged again and resuspended in buffer III. Then, the suspension was transferred to a Dounce homogenizer and homogenized with 20 strokes. The homogenized solution was centrifuged (3500 rpm, 5 minutes, 4°C) and the supernatant was transferred to a SS-34 tube and centrifuged. The supernatant transferred to a SS-34 tube again and centrifuged at 10 000 rpm for 10 minutes at 4°C to pellet mitochondria. The pellet was resuspended in 1 ml buffer III and protein concentration was measured at 280 nm. Aliquots of 10 mg/ml were stored at -80°C.

3.7 Pyrimidine Uptake of Isolated Mitochondria

To 100 µl of isolated mitochondria (10 mg/ml, solved in buffer III) 5 µl of H^3-TTP (15 Ci/mmol, Perkin Elmer) were added and the solution was incubated at 28°C for 10 minutes. Then, the solution was pipetted onto a glass fibre filter (Whatmann, 55 mm diameter, GFC) presoaked with buffer III while vacuum was applied. The filter was washed with 25 ml of

buffer III and placed into scintillation vial. 8 ml of LSC cocktail (Perkin Elmer Filter Count) were added and the emitted signal of the sample was measured by a scintillation counter.

3.8 Fe^{2+}-Uptake into Submitochondrial Particles (SMPs)

3.8.1 Preparation and Loading of SMPs

1 ml of mitochondria (10 mg/ml) were diluted 5-fold with 10 mM Tris pH 7.4, incubated on ice for 20 minutes and centrifuged at 27 000 rpm (for 10 minutes, 4°C, TLA 100.4). The pellet was resuspended in 1 ml of 250 mM sucrose, 10 mM Tris·HCl pH 7.4. The solution was sonicated three times for one minute at maximum intensity in an ice-bath and then centrifuged for 10 minutes at 10 000 rpm, 4°C. The supernatant was transferred to a new tube and centrifuged at 60 000 rpm for one hour, 4°C. The pellet was resuspended in 1 ml of 250 mM sucrose buffer, 10 mM Tris pH 7.4. For loading, 5 µl (50 µM) PhenGreen SK were added to the SMPs, they were sonicated three times for one minute and centrifuged for 10 minutes at 60 000 rpm, 4°C. The pellet was washed with 1 ml sucrose buffer, the centrifugation was repeated and the pellet was resuspended in 1 ml sucrose buffer.

3.8.2 Measuring the Fluorescence

The fluorescence was measured using the Perkin Elmer LS55 spectrofluorometer (FFA). Excitation and emission for PhenGreen SK were 506 and 520 nm. For measuring, 100 µl of loaded SMPs were diluted in 1.9 ml of sucrose buffer. 5 µM of an iron (II) solution and equal amounts of nucleotides were added to determine uptake.

3.9 Mg^{2+}-Uptake by Mag-Fura Measurements

3.9.1 Loading of Mitochondria and Measuring

Mitochondria (10 mg) were resuspended in 1 ml of buffer III containing ATP, pyruvic acid and succinic acid (100 ml buffer III, 0.2 g succinic acid, 0.01 g pyruvic acid, 0.03 g ATP). 30 µl of the acetoxymethyl (AM) ester form of mag-fura 2 (50 µg mag-fura 2-AM dissolved in 134.8 µl DMSO, purchased from Molecular Probes Inc.) and 5 µl Pluronic F-127 (100 µg pluronic dissolved in 250 µl DMSO, purchased from Molecular Probes Inc.) were added to the solution and incubated at 25°C shaking for 40 minutes to load the mitochondria with the dye. Then, the solution was centrifuged for two minutes at 10 000 rpm in a tabletop centrifuge, the supernatant was discarded and the mitochondria were resuspended in 1 ml buffer III containing ATP again. The solution was incubated another 40 minutes to allow the complete hydrolysis of the dye. After that, the samples were washed twice before measuring. For measuring ion concentrations, the spectroflourometer LS-55 (Perkin Elmer) with the fast

filter accessory (FFA), which allows fluorescence to be measured at 20 ms intervals with the excitation wavelength for mag-fura 2 at 340 and 380 nm and the emission wavelength at 509 nm, was used. All measurements were performed at 25°C in 3 ml cuvettets containing 2 ml solution (1 mg protein/ml) under stirring conditions. To analyze $[Mg^{2+}]_{ext}$-dependent changes in $[Mg^{2+}]_{int}$, external $[Mg^{2+}]$ is increased gradually to final concentrations of 1, 5 and 10 mM. Continuous recordings of fluorescent intensities at 340 nm and 380 nm were transformed into 340/380 wavelength ratios by using the computer program FL WinLab version 3.0 or 4.0. (Perkin Elmer) and $[Mg^{2+}]_{int}$ values were calculated from the 340/380-nm ratio according to the formula of Grynkiewicz *et al*. (1985) with a dissociation constant of the mag-fura 2/Mg^{2+} complex of 1.52 in buffer III. The minimum (R_{min}) and maximum (R_{max}) ratios were determined at the end of each experiment. R_{max} for mag-fura 2 was obtained by the addition of 10% SDS to lyse the cells. R_{min} was detected by the addition of 50 mM EDTA, pH 8, to remove all Mg^{2+} from the solution.

3.10 Protein Immunodetection

3.10.1 Growing and Harvesting of Cells and Mitochondria

Cells were grown in SD and YPD medium and mitochondria were prepared as described in 3.6.

3.10.2 Determination of Protein Concentration by Lowry

Protein concentration was determined with BIO-RAD *DC* kit (Lowry assay). Six standards of 0.2-1.2 mg/ml BSA in 1% SDS were prepared (total volume 50 µl). Working reagent A´ was prepared (20 µl reagent S/ml reagent A). The reactions were set up in Eppendorf tubes: to 25 µl of diluted sample (with 1% SDS) or reference 125 µl A´ were added and the solution was vortexed, then 1000 µl of reagent B were added and the solution was vortexed again. The reaction was transferred to fresh cuvettes and after 15 minutes the absorbance was read at 750 nm in the spectrophotometer (Hitachi U-2000).

3.10.3 SDS-PAGE

40 µg of protein were loaded onto a 10% bisacrylamide/acrylamide gel. The resolving gel and stacking gel were prepared according to Sambrook/Fritsch/Maniatis (Molecular Cloning. A Laboratory Manual, 2nd edition, 1989). The samples for loading were prepared in Eppendorf tubes, consisting of 40 µg of protein and filled up with 5% SDS to 10 µl, and 3 µl of 4×loading dye were added. The samples were heated for 5 minutes at 95°C and briefly centrifuged. The electrophoresis apparatus was filled with running buffer and the gel was loaded with the samples and marker (prestained PAGE RULER protein ladder, Fermentas).

Two gels were run at one time (20 mA/gel, 300V). Gels for Coomassie staining were incubated in staining solution and destained. After destaining, gels were washed in a 1% glycerine solution for 10 minutes and dried between transparent films.

3.10.4 Western Blot and Immunodetection

The sandwich for semi-dry blotting consisted of three layers of Whatmann paper soaked in transfer buffer, the nitrocellulose membrane soaked in transfer buffer, the gel and another three layers of Whatmann paper soaked in transfer buffer. The blot was run with 60mA/sandwich (15V) for 45 minutes (Bio Rad, Trans Blot® Semidry Transfer Cell).

The nitrocellulose membrane was incubated in blocking buffer (5% milk powder in TBS-T) overnight at 4°C. The membrane was washed three times for 10 minutes in TBS-T buffer at RT and incubated in anti-Rim2 antibody (1:5000, 2.5% milk powder in TBS-T, kindly provided by Prof. Fernando Palmieri, University of Bari, Department of Pharmaco-Biology) for two hours. After hybridisation, the membrane was washed three times for 10 minutes in TBS-T buffer and incubated with secondary antibody solution (horseradish peroxidase conjugated anti-chicken IgY 1:25 000, 2.5% milk powder in TBS-T, Sigma) for 1 hour. Washing steps were performed twice for 10 minutes in TBS-T and once in TBS buffer. For detecting the chemoluminescent signal, the SuperSignal® West Pico and Femto Maximum Sensitivity Substrates kits (Pierce) were used. Exposing times varied between 30 seconds and 10 minutes depending on the intensity of the signal.

4 Results

4.1 FET3-GFP assay

Yeast Mrs3/4p had previously been found to be involved in mitochondrial high-affinity iron uptake and were proposed to be the main mitochondrial iron transporters. However, other systems for iron import into yeast mitochondria are likely to exist, as the *mrs3/4*Δ phenotype only becomes evident on medium containing low iron. Recently, the pyrimidine nucleotide transporter Mrs12p had been shown to function as multi-copy suppressor of the *mrs3/4*Δ phenotype (Wiesenberger, unpublished results).

In order to investigate this surprising result and to find out if there indeed is a connection between Mrs12p and mitochondrial iron transport, we wanted, in a first attempt, to look at the expression of genes and proteins involved in iron uptake.

We chose to perform a *FET3*-GFP assay, as Fet3p, a ferro-O_2-oxidoreductase at the yeast cell surface, is part of the high-affinity iron uptake system and its transcription is strongly induced under conditions of low iron. Its expression is induced by Aft1p and Aft2p, which are inhibited by a signal from mitochondrial iron-sulfur clusters (Rutherford, Ojeda et al. 2005). Previous experiments have shown that the protein is up-regulated in *mrs3/4*Δ mutants. To test *FET3* expression in *mrs12*Δ and *mrs3/4/12*Δ cells, we transformed wild-type ρ^0 (Van Dyck, Jank et al. 1995), *mrs3/4*Δ ρ^0, *mrs12*Δ and *mrs3/4/12*Δ cells with a plasmid containing the *FET3*-GFP construct under its endogenous promoter, grew the cells in medium containing high iron concentrations to ensure that induction of *FET3* would be due to the diminished mitochondrial iron uptake and not to the absence of iron in the cell and checked GFP emission of equal cell amounts at 510 nm.

As displayed in **Figure 3**, *FET3* expression in *mrs3/4*Δ cells was about three times higher than in wild-type cells. *mrs12*Δ cells showed no significant increase in *FET3* expression compared to the wild-type, indicating that the high-affinity iron uptake system was not turned on by Aft1p and the *mrs12*Δ mitochondria did not sense iron deprivation. *mrs3/4/12*Δ cells, however, displayed the highest induction of *FET3*, meaning that even less iron was available in their mitochondria than in *mrs3/4*Δ and that Mrs12p contributes to iron availability in mitochondria, but this effect is only visible in the *mrs3/4/12*Δ mutant.

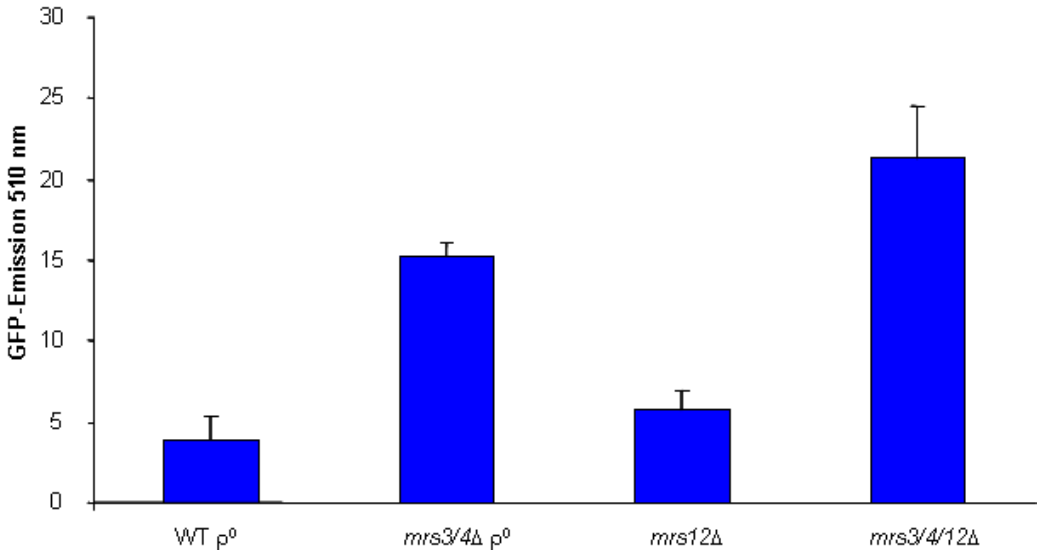

Figure 3: *FET3*-GFP expression is induced to a higher extent in *mrs3/4/12*Δ cells than in *mrs3/4*Δ ρ^0 cells. W303 ρ^0 and GW400 ρ^0 (*mrs3/4*Δ) transformed with *FET3*-GFP were grown in SD -Ura medium supplemented with ferric ammonium citrate (50 µg/ml) to early logarithmic phase and diluted to an OD of 1. GFP-emission was measured at 510 nm. Standard deviations were calculated from four independent experiments.

4.2 Gene expression profiling of mrs3/4/12Δ

As the *FET3*-GFP did not show up-regulation of *FET3* in *mrs12*Δ cells, we decided to perform gene expression profiling of *mrs12*Δ and *mrs3/4/12*Δ and compare them to W303 ρ^0 cells to see if other genes involved in cellular iron-uptake would be found to be up-regulated.

As presented in **Table 3**, several genes belonging to the iron regulon were up-regulated in the *mrs3/4/12*Δ mutant. These genes are involved in iron or siderophore-iron transport (*FTR1*; *FIT2*, *FIT3*), in the degradation of heme (*HMX1*) or act as transcription factor containing an Aft1p consensus motif (*TIS11*) (Shakoury-Elizeh, Tiedeman et al. 2004; Puig, Askeland et al. 2005).

Another up-regulated gene was *SLA1*, its gene product functions as a cytoskeletal protein binding protein, which is required for the assembly of the cortical actin cytoskeleton. Its induction might be due to increased stress in the triple mutant.

Down-regulated genes include the oxalacetate carrier (*OAC1*), cytochrome c_1 (*CYT1*) and a subunit of cytochrome c oxidase (*COX5*a). These genes code for mitochondrial proteins, which are likely to be down-regulated in cells with defects in mitochondrial proteins. Another down-regulated gene was dihydroorotate dehydrogenase (*URA1*), its protein product is located in the cytoplasma and catalyzes the fourth step in the *de novo* biosynthesis of pyrimidines. The reason for its down-regulation might be that pyrimidines are not transported

into mitochondria in cells lacking Mrs12p and therefore Ura1p is not needed to synthesize them *de novo*.

Name	Gene	Induction	Function
Iron homeostasis			
FIT2	**YOR382W**	1.9	Iron transport
FTR1	**YER145C**	1.2	Iron transport
HMX1	**YLR205C**	1.0	Heme-binding peroxidase involved in the degradation of heme, expression regulated by Aft1p
TIS11	**YLR136C**	1.3	Putative transcription factor, Aft1p consensus motif
FIT3	**YOR383C**	2.7	Iron transport
Others			
SLA1	**YBL007C**	1.9	Actin cytoskeleton

Name	Gene	Induction	Function
OAC1	**YKL120W**	-2.2	Oxalacetate carrier, sulfate porter
CYT1	**YOR065W**	-2.8	Cytochrome c_1
COX5A	**YNL052W**	-2.0	Subunit Va of cytochrome c oxidase
URA1	**YKL216W**	-1.4	Dihydroorotate dehydrogenase, involved in de novo biosynthesis of pyrimidines

Table 3: Genome wide expression profile of W303 *mrs3/4/12*Δ cells shows up-regulation of genes involved in iron homeostasis. W303 ρ^0 (wild-type) and OS1-2d (*mrs3/4/12*Δ) were grown in SD complete medium overnight, diluted to an OD_{600} = 0.3 and grown to an OD_{600} of 1.5. RNA isolation, cDNA generation, and probe cleanup and microarray hybridization were performed as described in materials and methods. Microarrays were read using an Axon GenePix 400B laser scanner and analyzed using the GenePix Pro 3.0 software. Experiments were repeated three times with independent cultures.

In *mrs12*Δ cells, *FIT2* and *FIT3*, two genes of the iron regulon, are induced (data are presented in **Table 4** by permission of Dr. Jochen Stadler). Fit2p and Fit3p are located in the cell wall and are involved in the retention of siderophore-iron. Down-regulated genes include pyruvate decarboxylase (*PDC1*/*PDC6*), cytosolic aldehyd dehydrogenase (*ALD6*), phosphatidate cytidyltransferase (*CDS1*) and α-isopropylmalate synthase (*LEU4*).

Comparing the gene expression profiles of *mrs12*Δ and *mrs3/4/12*Δ to wild-type cells, it can be seen that in both *FIT2* and *FIT3* are induced, indicating a role of *mrs12*Δ in mitochondrial iron acquisition. However, when compared to Mrs3/4p, deletion of Mrs12p only has a minor effect on the expression of the iron regulon. As can be seen in the *mrs3/4/12*Δ mutant, several other genes involved in iron transport and homeostasis besides *FIT2* and *FIT3* are induced, which is due to the absence of Mrs3/4p, the main mitochondrial iron transporters.

Name	Gene	Induction	Function
Iron homeostasis			
FIT2	**YOR382W**	3.5	Iron transport
FIT3	**YOR383W**	3.1	Iron transport

Name	Gene	Induction	Function
PDC6	YGR087C	-2.6	Pyruvate decarboxylase, isoform
PDC1	YLR044C	-1.9	Pyruvate decarboxylase, isoform
ALD6	YPL061W	-1.8	Cytosolic aldehyde dehydrogenase

Table 4: Genome wide expression profile of W303 *mrs12*Δ shows up-regulation of genes involved in iron homeostasis. W303 ρ^0 (wild-type) and OS1-2d (*mrs12*Δ) were grown in SD complete medium overnight, diluted to an OD_{600} = 0.3 and grown to an OD_{600} of 1.5. RNA isolation, cDNA generation, and probe cleanup and microarray hybridization were performed as described in materials and methods. Microarrays were read using an Axon GenePix 400B laser scanner and analyzed using the GenePix Pro 3.0 software. Experiments were repeated three times with independent cultures.

4.3 Construction and analysis of mrs12 *G245Y S246A*

4.3.1 Construction of *mrs12* G245Y S246A by *in vitro* mutagenesis

Mrs12p is, like Mrs3p and Mrs4p, a member of the mitochondrial carrier family. Recently, the x-ray structure of the bovine mitochondrial carrier protein ADP/ATP translocase had been published (Pebay-Peyroula, Dahout-Gonzalez et al. 2003). Subsequent computational analysis and comparative modeling revealed a common binding site for the substrates of the mitochondrial carrier proteins (Kunji and Robinson 2006) and the amino acids at the three contact points of the binding site have been determined by sequence alignment for all carriers. These findings enabled us to create a mutant of *MRS12* in the proposed contact point II in order to investigate the involvement of this contact point in *MRS12* function. We were further interested in studying the role pyrimidine transport might play in suppressing the *mrs3/4*Δ phenotype, as iron transport into *mrs3/4*Δ submitochondrial particles (SMPs) overexpressing *MRS12* is only seen when pyrimidines are added together with iron (Froschauer, unpublished results), whereas previous experiments showed that iron is readily taken up into wild-type SMPs, but not in SMPs lacking Mrs3/4p (Froschauer, in press).

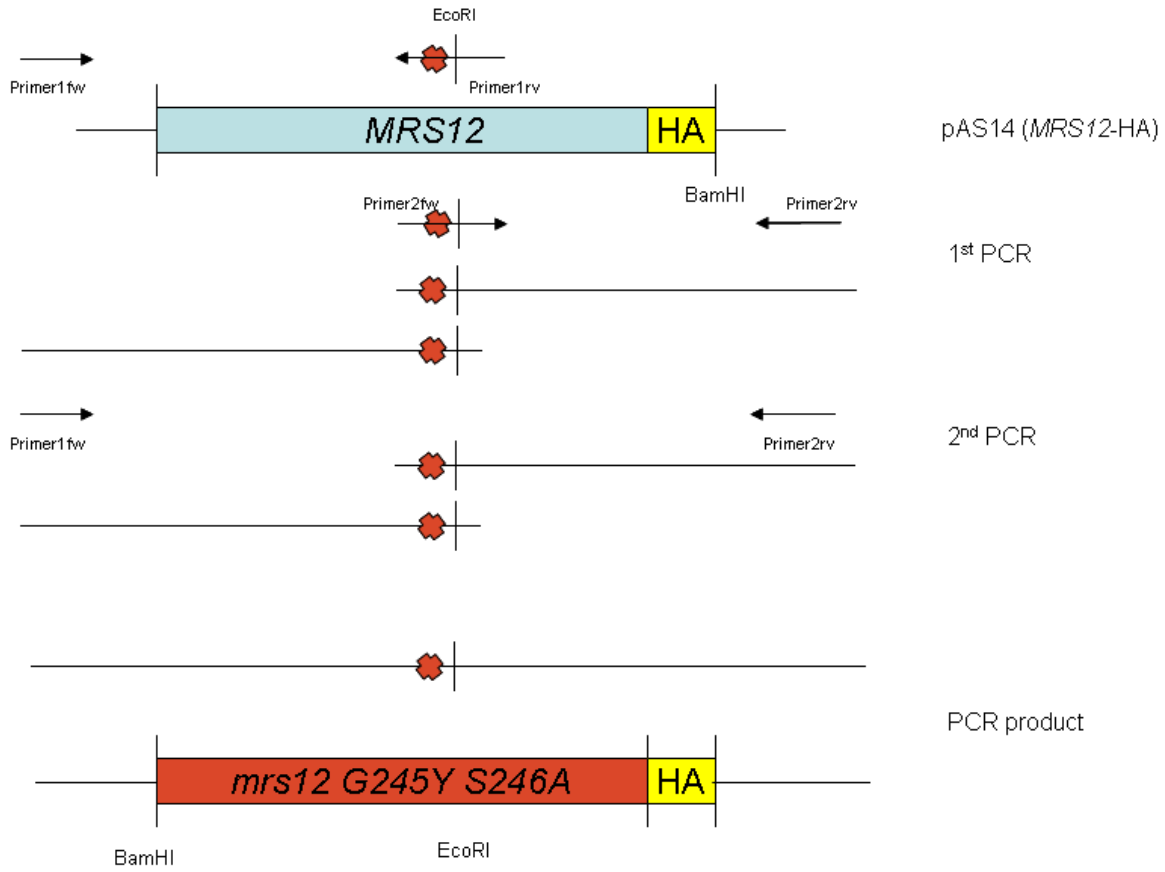

Figure 4: Construction of the PCR product containing the *mrs12* G245Y S246A gene by *in vitro* mutagenesis. The vector pAS14 (*MRS12*-HA) was used as template. The 1st PCR was run with primers containing base changes in the regions of interest (indicated by ×) and a silent EcoRI restriction site (indicated by |) (primer1rv or primer2fw) and outside primers (primer1fw or primer2rv). The 2nd PCR was run with outside primers and the two products from the 1st PCR to obtain the PCR product.

We decided to mutate the amino acids glycine (G245) and serine (S246) at contact site II of Mrs12p into tyrosine and alanine as these two amino acids have very different chemical sizes and features and are therefore likely to interfere with normal substrate recognition. Primers containing the mutations GGTTCT → TATGCT inside the *MRS12* gene sequence were constructed together with a silent EcoRI restriction site (GTATAC → GAATTC) to identify desired clones. Outside primers were placed in the polylinker regions of the template plasmid (pAS14, see appendix for plasmid maps). pAS14 contained the *MRS12* gene with a C-terminal HA-tag, the HA-tag is not functional in the protein (Wiesenberger, personal communication), but can be used for protein detection with anti-HA antibody (see **Figure 4**).

The PCR product was cut with BamHI and cloned into the mulit-copy plasmid pAS14 (*MRS12*-HA). The vector containing the desired insertion was identified by digestion with EcoRI (**Figure 5**) and called pMH1 (*mrs12* G245Y S246A-HA).

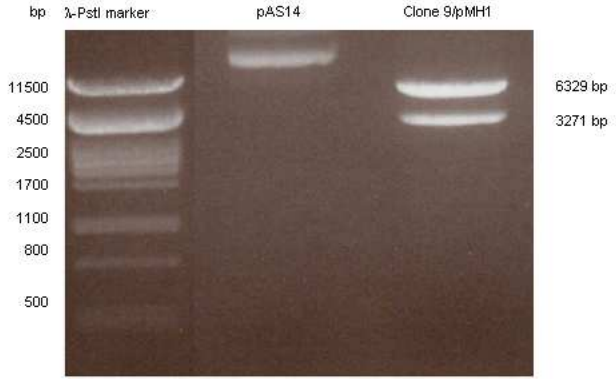

Figure 5: A second EcoRI restriction site is detected for the vector pMH1 (clone 9), indicating that it contains the *mrs12* G245Y S246A mutation. Vector pAS14 and clone 9/pMH1 were cut with EcoRI and loaded onto a 1% agarose gel for analysis.

Then, pMH1 was cut with NotI and religated to lose the HA-tag, the resulting vector was called pMH2 (**Figure 6**).

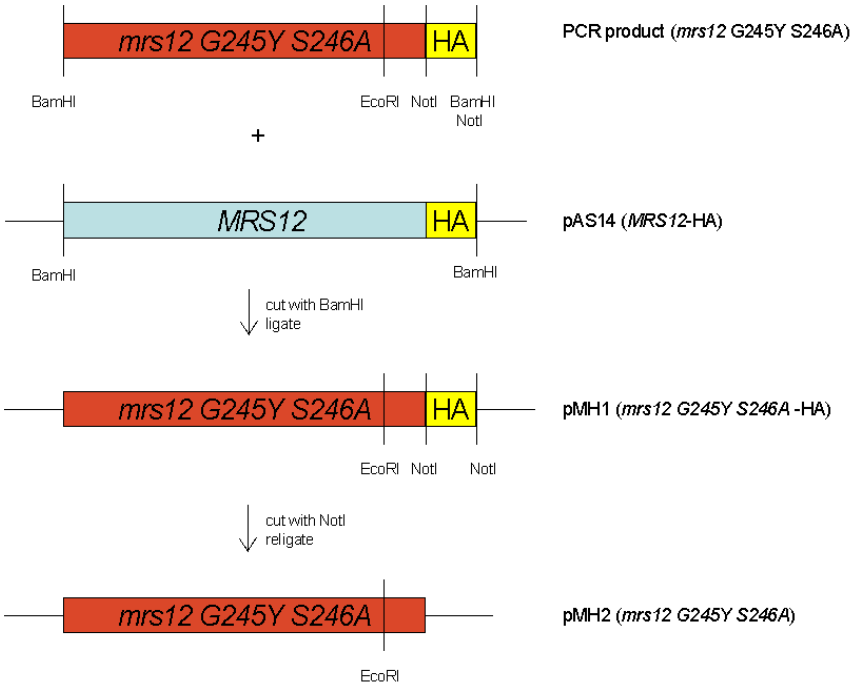

Figure 6: Construction of vectors pMH1 (*mrs12* G245Y S246A-HA) and pMH2 (*mrs12* G245Y S246A). The PCR product was cut with BamHI and cloned into vector pAS14. The resulting vector was called pMH1. pMH1 was cut with NotI and religated to get rid of the HA-tag. This vector was called pMH2.

To obtain a single-copy plasmid with *mrs12* G245Y S246A under its endogenous promoter, the *mrs12* G245Y S246A gene from pMH2 was cloned into the single-copy vector pOLU2 (YCplac33 backbone), which contained the *MRS12* gene under its own promoter. The resulting vector was called pMH5 (**Figure 7**). The vector pMH2 and its low-copy analogue pMH5 were used in this work for studying *mrs12* G245Y S246A function.

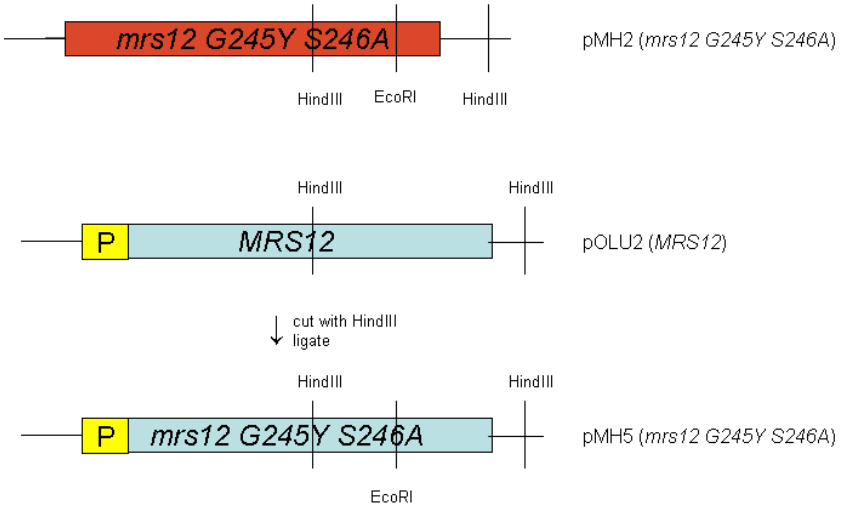

Figure 7: Construction of vector pMH5 (*mrs12* G245Y S246A, endogenous promoter). Vector pMH2 was cut with HindIII and the fragment with *mrs12* G245Y S246A was cloned into vector pOLU2, which contained the *MRS12* gene under its endogenous promoter. Correct orientation of the insert was verified by restriction digestion and the resulting vector was called pMH5.

4.3.2 Complementation studies

In order to find out if *mrs12* G245Y S246A was functional and could complement the *mrs12*Δ phenotype, complementation studies were performed. The *mrs12*Δ phenotype manifests itself by loss of mitochondrial DNA and slow growth on glucose compared to ρ^0 wild-type cells, therefore cells lacking *MR12* form comparatively smaller colonies than isogenic wild-type ρ^0 cells. To avoid mitochondrial DNA loss when comparing phenotypes, the diploid strain YAS1(*MRS12*/*mrs12*Δ) was transformed with plasmids YCplac33, pMH3 (*MRS12*.YCplac33) and pMH5 (*mrs12* G245Y S246A.YCplac33), transformants were sporulated, tetrads dissected and replica-plated onto YPD (to obtain the phenotype), onto SD –Ura (to determine which tetrads contain plasmids), onto YPD supplemented with the antibiotic geneticin (to select for *mrs12*Δ colonies) and JJ1A and JJ1C plates (to determine the mating type). Under regular segregation, it is expected that a tetrad deriving from a diploid *MRS12*/*mrs12*Δ contains two colonies, which carry wild-type *MRS12* and show normal growth, and two colonies without *MRS12*, which show reduced growth. As seen in **Figure 8**, this expected 2:2 segregation was observed for cells transformed with the empty plasmid

YCplac33. On the other hand, cells transformed with the single-copy plasmid *MRS12*.YCplac33 (pMH3) did not show this segregation pattern, here all colonies had normal growth as the *MRS12* gene on the plasmid complemented the two tetrads with *mrs12*Δ. By comparing transformants with single-copy *mrs12* G245Y S246A.YCplac33 (pMH5) with the controls, it is evident that these tetrads show a 2:2 segregation.

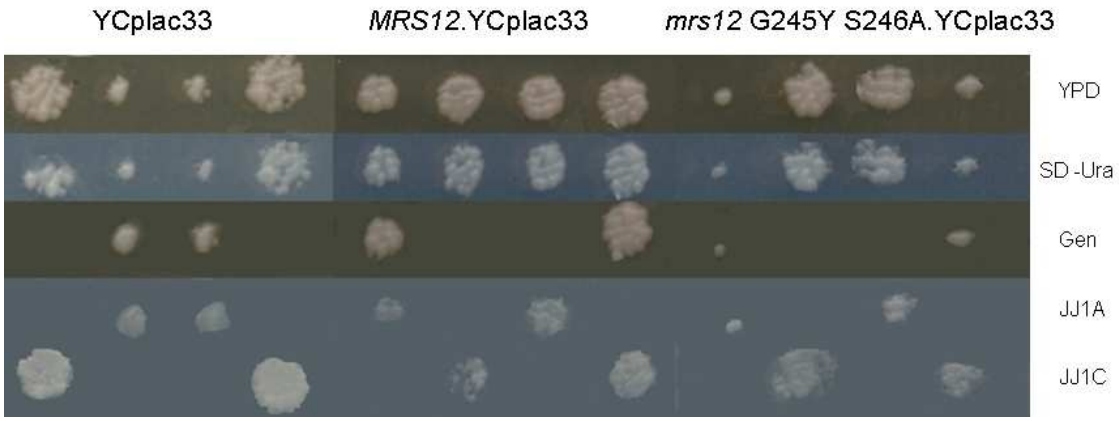

Figure 8: *mrs12* G245Y S246A does not support complementation of a *mrs12*Δ mutant. Diploid YAS1 (*MRS12*/*mrs12*Δ) was transformed with YCplac33, with pMH3 (*MRS12*.YCplac33) and with pMH5 (*mrs12* G245Y S246A.YCplac33). Transformants were sporulated and tetrads were dissected. Tetrads were replica-plated onto YPD, SD –Ura, YPD + geneticin (200 µg/ml), a lawn of JJ1A (mating type a) and a lawn of JJ1C (mating type α).

The reduced growth rate of transformants carrying *mrs12* G245Y S246A.YCplac33 could also be observed in growth tests, as displayed in **Figure 9**. From these results, it is obvious that the mutated *mrs12* G245Y S246A is not able to complement the *mrs12*Δ phenotype and that it is therefore not functional.

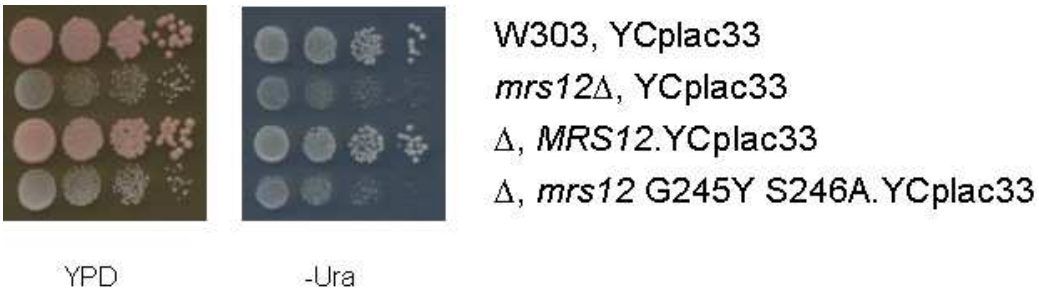

Figure 9: Complementation of the *mrs12*Δ phenotype is achieved by *MRS12*, but not by *mrs12* G245Y S246A. Segregants carrying YCplac33 (W303, *mrs12*), *MRS12*.YCplac33 (*mrs12*Δ), *mrs12* G245Y S246A.YCplac33 (*mrs12*Δ) (all mating type a) were grown in SD –Ura overnight. After cultures were prepared and transfered onto YPD and SD –Ura plates complementation of the *mrs12*Δ phenotype by *MRS12*.YCplac33 and by *mrs12* G245Y S246A.YCplac33 was compared.

4.3.3 Radioactive ^{3}H-TTP uptake into isolated mitochondria

To further test if pyrimidine transport by *MRS12* is impaired in mitochondria carrying *mrs12* G245Y S246A, mitochondria were incubated with radioactive ^{3}H-TTP and uptake was measured by scintillation counting. In **Figure 10**, it can be seen that wild-type ρ^{0} mitochondria and *mrs12*Δ mitochondria overexpressing *MRS12* showed about two-fold higher uptake than *mrs12*Δ mitochondria, whereas uptake was not elevated in *mrs12*Δ mitochondria overexpressing *mrs12* G245Y S246A compared to the *mrs12*Δ mitochondria. When bathophenanthrolinedisulfonate, an inhibitor of Mrs12p (Marobbio, Di Noia et al. 2006), was added to wild-type ρ^{0} and *mrs12*Δ mitochondria overexpressing *MRS12*, the uptake was reduced to *mrs12*Δ level. In the case of *mrs12*Δ mitochondria and *mrs12*Δ mitochondria overexpressing *mrs12* G245Y S246A, addition of bathophenanthrolinedisulfonate did not significantly reduce pyrimidine uptake. These observations indicate that pyrimidine uptake is impaired in *mrs12* G245Y S246A mitochondria and that the mutation in contact point II indeed affects the transport function of the protein.

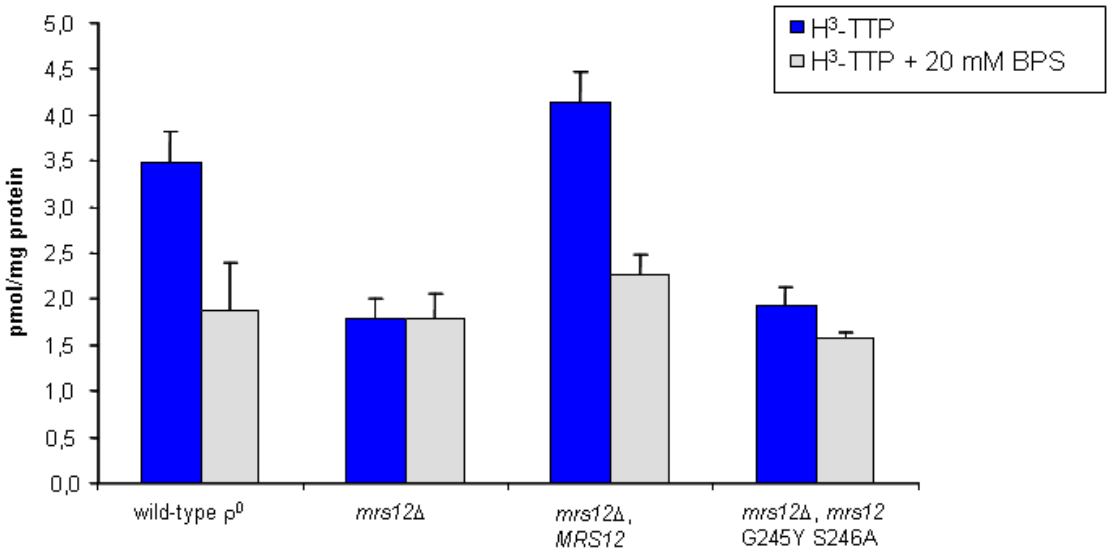

Figure 10: Mitochondria lacking Mrs12p or carrying Mrs12p G245Y S246A do not take up pyrimidines. Mitochondria isolated from yeast strain DBY ρ^{0} or isogenic mutant strains were incubated with radioactive labelled ^{3}H-TTP (15 Ci/mmol) or with ^{3}H-TTP and inhibitor bathophenanthroline (20 mM) for 10 minutes, filtered through a glass fibre filter and washed with 0.6M sorbitol/20 mM Tris·HCl pH 7.4. The filter was put into a scintillation vial, scintillation cocktail was added and scintillation of the sample was counted.

4.4 MRS12 and iron transport

4.4.1 Suppression of the *mrs3/4*Δ phenotype by overexpression of *MRS12* or *mrs12* G245Y S246A

The *mrs3/4*Δ phenotype shows reduced growth on YPD at 37°C, on YPG, on media with low iron concentrations and on media supplemented with Cd^{2+}. To test if pyrimidine transport, Mrs12p's assigned function, is essential to suppress the *mrs3/4*Δ phenotype, *mrs3/4*Δ cells were transformed with plasmid pMH2 carrying the *mrs12* G245Y S246A mutation and compared with wild-type, *mrs3/4*Δ mutant and *mrs3/4*Δ mutant transformed with wild-type *MRS12*. Growth tests clearly showed that *mrs3/4*Δ cells carrying *MRS12* on a multi-copy plasmid grew as well on all plates as the wild-type, whereas *mrs3/4*Δ cells and *mrs3/4*Δ cells transformed with *mrs12* G245Y S246A showed reduced or no growth at all (see **Figure 11**). This demonstrates that the *mrs12* G245Y S246A mutant cannot suppress the *mrs3/4*Δ phenotype and that functional *MRS12* is needed for suppression.

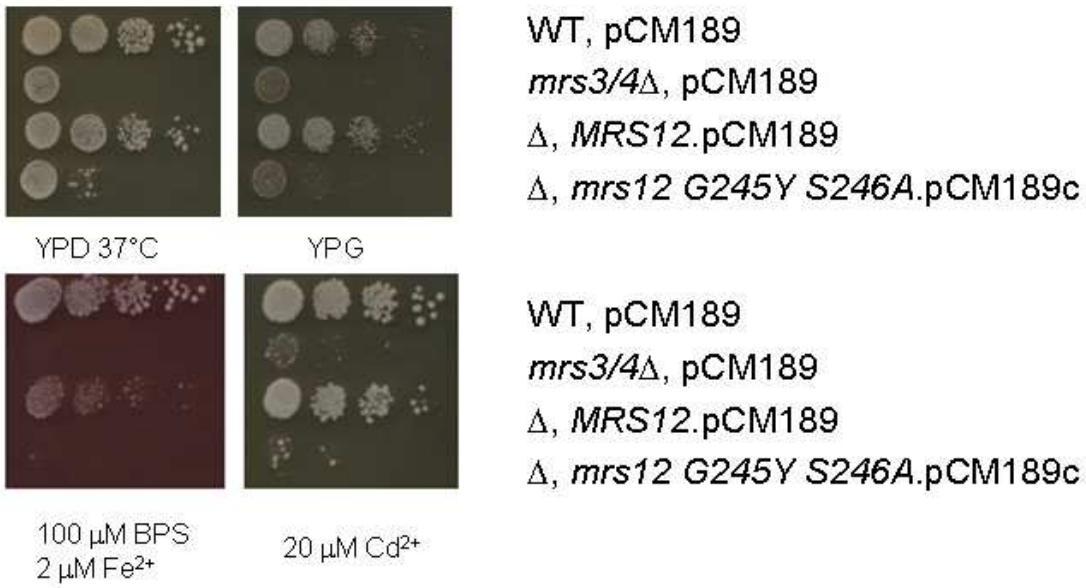

Figure 11: *MRS12* overexpression suppresses the *mrs3/4*Δ phenotype, whereas *mrs12* G245Y S246A overexpression does not. DBY474 (wild-type) and GW403 (*mrs3/4*Δ) were transformed with pCM189 and *mrs3/4*Δ cells with *MRS12*.pCM189 or *mrs12* G245Y S246A.pCM189. Transformants were grown in SD –Ura medium to an OD_{600} of 1, diluted and transferred onto YPD, YPD with reduced iron content (supplemented with 100 µM of the iron chelator bathophenanthrolinedisulfonate (BPS) and 2 µM Fe^{2+}), YPD with cadmium or YPG to obtain the *mrs3/4*Δ phenotype.

4.4.2 Immunodetection of *MRS12* and *mrs12* G245Y S246A

To control Mrs12p and Mrs12p G245Y S246A expression from multi-copy plasmids, anti-Rim2-antibody was used to detect the proteins in mitochondrial extracts. Blots and coomassie stained gel are shown in **Figure 12**. No signal was obtained for wild-type and *mrs3/4*Δ mutant, the normal Mrs12p expression level seems to be below detection level of the antibody. For cells overexpressing *MRS12* or *mrs12* G245Y S246A, signals were detected for both proteins at about 42 kDa. Hence, it can be concluded that the Mrs12p G245Y S246A mutant is not degraded and that lack of *mrs3/4*Δ suppression is probably due to a non-functional protein. As shown by the Coomassie gel, equal amounts of protein (40 µg) were loaded into each lane.

In the case of the W303-1A strain, whole cell extracts could be used to obtain a signal by western blotting. *MRS12* expression from the plasmids seems to be induced to a higher extent or Mrs12p is degraded to a lesser extent in this strain than in DBY747, as for the latter mitochondrial extracts had to be used to detect Mrs12p signals.

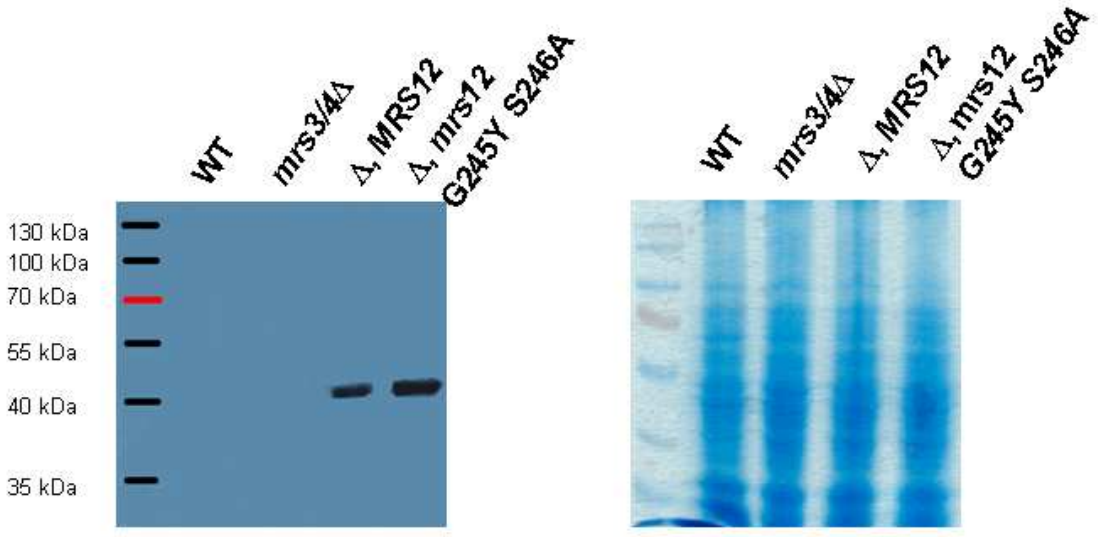

Figure 12: Mrs12p and Mrs12 G245Y S246Ap are detected by anti-Mrs12p-antibody in mitochondrial extracts of *mrs3/4*Δ cells. Mitochondria were isolated from yeast strains DBY747 (wild-type) and GW403 (*mrs3/4*Δ) and protein concentrations were determined with the Lowry Method. 40 µg of each protein extract were loaded onto a 12% bisacrylamide/acrylamide gel, the gel was run and proteins were transferred onto a nitrocellulose membrane. The membrane was incubated with anti-Mrs12-antibody solution and secondary antibody solution as described in materials and methods.

4.4.3 Iron uptake into submitochondrial particles by *MRS12* and *mrs12* G245Y S246A

To study iron uptake across the inner mitochondrial membrane by Mrs12p *in vitro*, submitochondrial particles (SMPs) were used. Submitochondrial particles are generated from mitochondria by exposing these organelles to low osmolarity buffer to generate mitoplasts, which lack the outer mitochondrial membrane, and then to ultrasound. This causes fragmentation of the mitoplasts and the inner mitochondrial membrane is turned inside out. The residual membrane still contains active mitochondrial membrane proteins and can be used to determine ion uptake by loading the SMPs with specific fluorescent dyes. These dyes act as ion chelators and change their fluorescent emission when they bind ions. For iron measurements, the dye PhenGreen SK was used, which shows quenching of fluorescent emission at 520 nm upon iron binding. In the following experiments, SMPs deriving from wild-type cells, *mrs3/4*Δ cells, *mrs3/4*Δ cells overexpressing *MRS12* and *mrs3/4*Δ cells overexpressing *mrs12* G245Y S246A were studied.

After addition of Fe^{2+} to wild-type SMPs quenching was clearly observed, indicating that the dye binds the metal inside the SMPs, as wild-type SMPs are able to transport iron across the membrane. However, when the main iron transporters Mrs3/4p are absent, no change in fluorescent emission was detected, showing that *mrs3/4*Δ SMPs do not take up iron. In *mrs3/4*Δ SMPs containing high-copy numbers of Mrs12p, iron uptake was observed, but only upon prior addition of CTP or TTP, no uptake was seen without CTP/TTP. As shown in **Figure 13**, the amount of iron uptake is dependent on the concentration of the pyrimidine nucleotides, higher uptake is detected for increasing concentrations of the nucleotides.

In *mrs3/4*Δ SMPs carrying high-copy numbers of the Mrs12p G245Y S246A mutant, iron uptake was significantly decreased upon addition of TTP and CTP when compared to *mrs3/4*Δ SMPs with high-copy numbers of Mrs12p (**Figure 14**). This shows that iron does not enter SMPs via Mrs12p without pyrimidine co-transport.

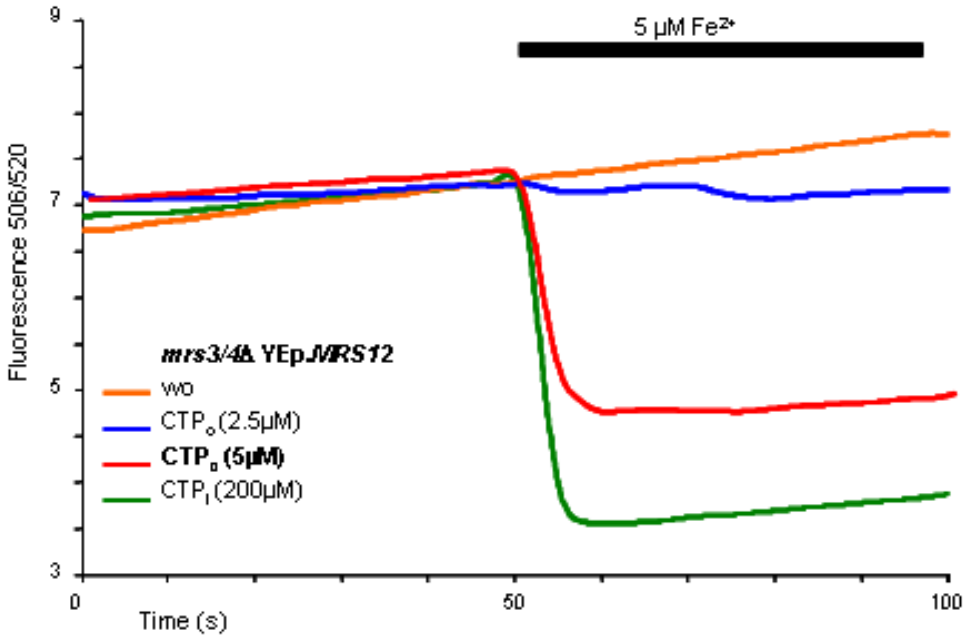

Figure 13: Addition of pyrimidine nucleotides stimulates iron uptake into *mrs3/4*Δ submitochondrial particles (SMPs) carrying high-copy numbers of Mrs12p. Mitochondria were isolated from GW403 *mrs3/4*Δ strain overexpressing *MRS12*, SMPs were prepared and loaded and the fluorescence was measured as described in materials and methods.

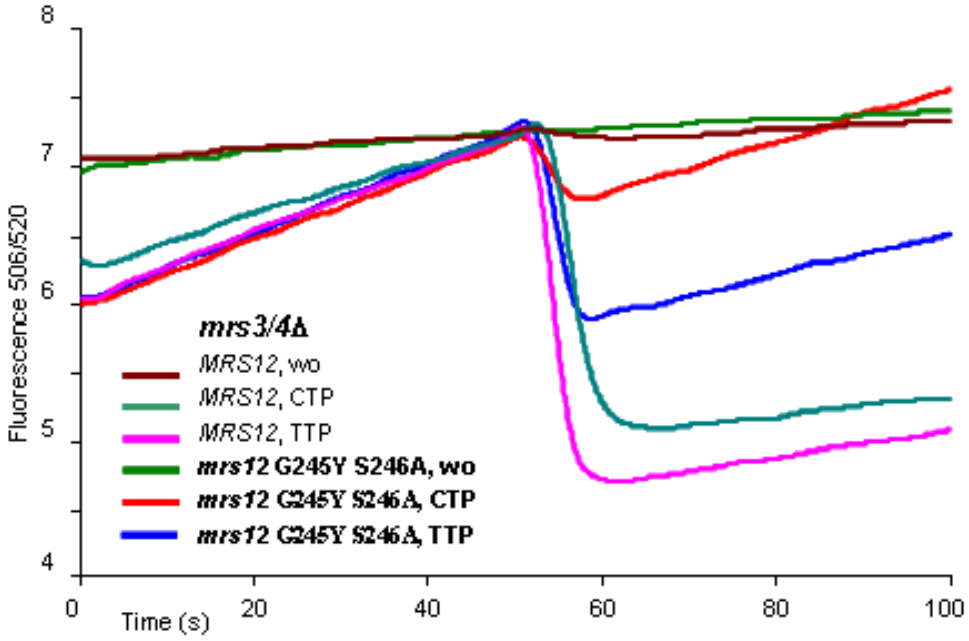

Figure 14: Upon addition of pyrimidine nucleotides *mrs3/4*Δ SMPs carrying high-copy numbers of Mrs12p G245Y S256A show decreased iron uptake. Mitochondria were isolated from GW403 *mrs3/4*Δ strain overexpressing *MRS12* or *mrs12* G245Y S246A, SMPs were prepared and loaded and the fluorescence was measured as described in materials and methods.

Taken together, these *in vitro* data show that iron is transported into SMPs by Mrs12p, but transport only takes place when pyrimidines are present and when Mrs12p is able to carry out pyrimidine transport.

4.5 MRS12 and Mg^{2+}-transport

4.5.1 Suppression of the *mrs2*Δ phenotype by overexpression of *MRS12* or *mrs12* G245Y S246A

So far, we could show that iron was transported along with pyrimidines by Mrs12p. In a next step, we assumed that other divalent ions could be taken up together with pyrimidines as well. To study this expectation, we chose a strain lacking the *MRS2* gene. This gene has been identified in a screen for multicopy suppressors of a mitochondrial RNA splicing defect and is a mitochondrial inner membrane protein which shares high sequence similarity with the bacterial Mg^{2+} transporter CorA (Bui, Gregan et al. 1999). It functions as the main mitochondrial Mg^{2+} transporter (Kolisek, Zsurka et al. 2003). The *mrs2*Δ phenotype shows reduced growth on media lacking fermentable carbon-sources, but can be suppressed by overexpression of several proteins of the inner mitochondrial membrane, including the members of the mitochondrial carrier family *MRS3* and *MRS4*.

Here, it could be observed in growth tests using the DBY747 strain that overexpression of *MRS12* suppressed the *mrs2*Δ phenotype on YPG. Consistent with the findings above, no suppression was seen for the *mrs12* G245Y S246A mutant. For the W303 strain only a slight phenotype was seen on YPG and overexpression of *mrs12* G245Y S246A resulted in a stronger suppression of *mrs2*Δ than observed in the DBY747 strain (**Figure 15**). As demonstrated for the *mrs3/4*Δ phenotype, overexpression of *MRS12* could also compensate for the absence of Mrs2p, the mitochondrial Mg^{2+} transporter, showing that Mrs12p is also able to transport other divalent metals than iron into mitochondria.

4.5.2 Immunodetection of *MRS12* and *mrs12* G245Y S246A

Mrs12p and Mrs12p G245Y S246A were both detected in mitochondrial extracts of cells overexpressing *MRS12* or *mrs12* G245Y S246A by anti-Rim2 antibody. No signals were obtained for wild-type or *mrs2*Δ cells, which do not overexpress *MRS12*. The detected proteins had a size of about 42 kDa, the mutant Mrs12p G245Y S246A was stably expressed and not degraded (**Figure 16**). Therefore, lack of *mrs2*Δ suppression is due to a non-functional protein. As shown by the Coomassie gel, equal amounts of protein (40 µg) were loaded into each lane.

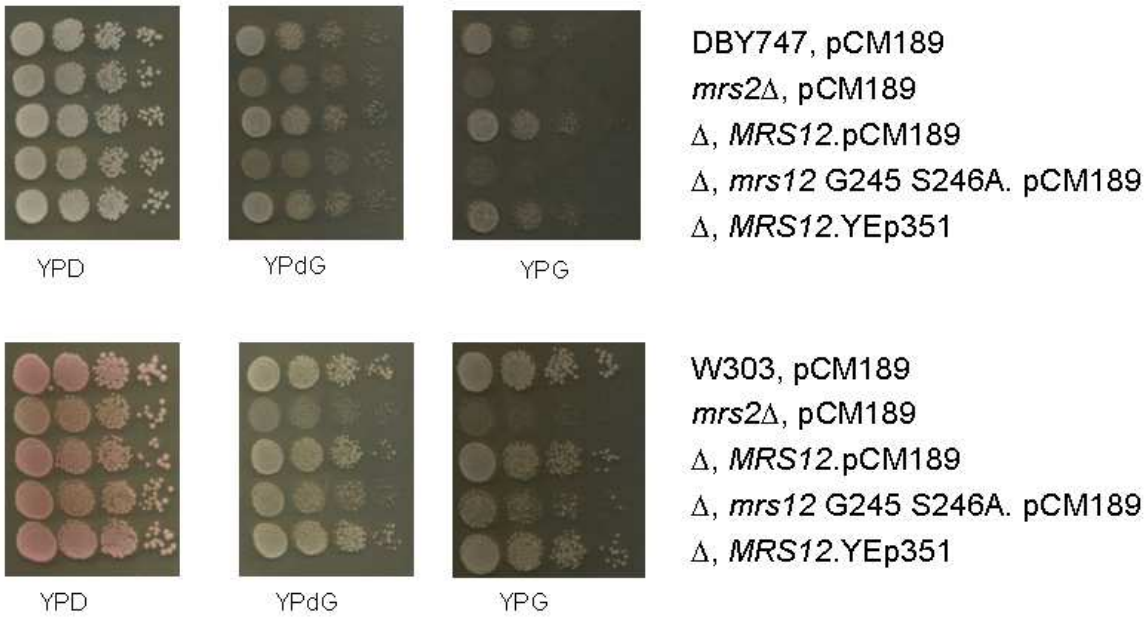

Figure 15: *MRS12* overexpression suppresses the *mrs2*Δ phenotype, whereas *mrs12* G245Y S246A does not. DBY747 and W303 (wild-type) and isogenic *mrs2*Δ cells were transformed with pCM189 and *mrs2*Δ cells with *MRS12*.pCM189, *mrs12* G245Y S246A.pCM189 or *MRS12*.YEp351. Transformed cells were grown in SD -Ura to an OD_{600} of 1 and plated onto YPG or YPdG to obtain the *mrs2*Δ phenotype.

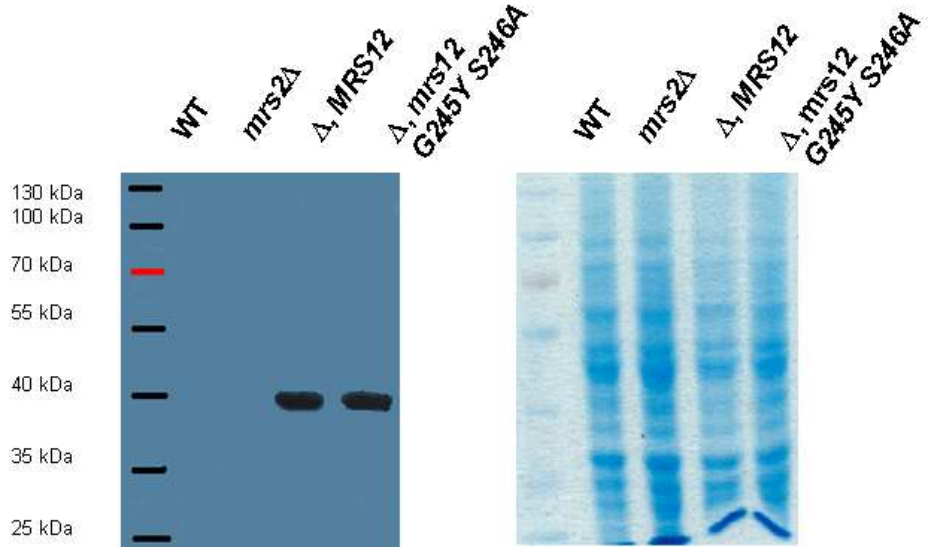

Figure 16: Mrs12p and Mrs12p G245Y S246Ap are both detected by anti-Mrs12p-antibody in mitochondrial extracts of *mrs2*Δ cells. Mitochondria were isolated from yeast strains and protein concentrations were determined with the Lowry Method. 40 µg of each protein extract were loaded onto a 12% bisacrylamide/acrylamide gel, the gel was run and the proteins were transferred onto a nitrocellulose membrane. The membrane was incubated in anti-Mrs12-antibody solution and secondary antibody solution as described in materials and methods.

4.5.3 Mg^{2+}-uptake into isolated mitochondria

For *in organello* Mg^{2+}-uptake studies, mitochondria were isolated and incubated with the fluorescent dye mag-fura 2. Mag-fura 2 is a membrane permeant acetomethoxyl ester, which becomes membrane-impermeant and Mg^{2+}-sensitive upon hydrolysation by mitochondrial non-specific esterases. When Mg^{2+} is bound by the dye, the fluorescent intensities at 340 and 380 nm change and, according to the following formula (Grynkiewicz, Poenie et al. 1985), the 340/380 wavelength ratio can be used to calculate $[Mg^{2+}]_i$ values:

$$K_D \cdot \frac{F_O}{F_S} \cdot \frac{R - R_{min}}{R_{max} - R} = [Mg^{2+}]$$

R is the ratio of the fluorescence at 340 nm and the fluorescence at 380 nm, R_{min} and R_{max} are the 340 nm/380 nm ratios at 0 and 30 mM Mg^{2+}, K_D is the effective dissociation constant of the mag-fura 2/Mg^{2+} complex in breaking buffer (which was determined as 1.52 mM), and F_0 and F_S are the 380 nm excitation efficiencies in 0 mM Mg^{2+} and at saturating Mg^{2+} (30 mM).

Upon addition of 1 mM, 5 mM and 10 mM Mg^{2+} to wild-type mitochondria, an increase in the fluorescence at 340 nm and a decrease in the fluorescence at 380 nm were observed, reflecting an increase in internal Mg^{2+}. Only minor increase in $[Mg^{2+}]_i$ was detected in *mrs2*Δ mitochondria due to the absence of the main mitochondrial Mg^{2+} transporter Mrs2p. In *mrs2*Δ mitochondria with high-copy numbers of Mrs12p $[Mg^{2+}]_i$ increased compared to *mrs2*Δ, but did not equal wild-type level. *mrs2*Δ mitochondria containing Mrs12p G245Y S246A displayed Mg^{2+}-uptake in a concentration range between *mrs2*Δ and *mrs2*Δ overexpressing *MRS12* mitochondria (see **Figure 17** and **Figure 18**).

In a further experiment, we also tried to add pyrimidine nucleotides together with Mg^{2+} to *mrs2*Δ *MRS12* mitochondria to check whether this would stimulate uptake, but as the pyrimidines complexed a certain amount of Mg^{2+} and therefore were competing with mag-fura 2, exact determination of $[Mg^{2+}]_i$ via R_{max} and R_{min} ratios was not possible.

However, these findings show that Mrs12p is able to promote Mg^{2+} uptake and that pyrimidine nucleotide transport plays a role in the protein's ability to suppress the *mrs2*Δ mutation.

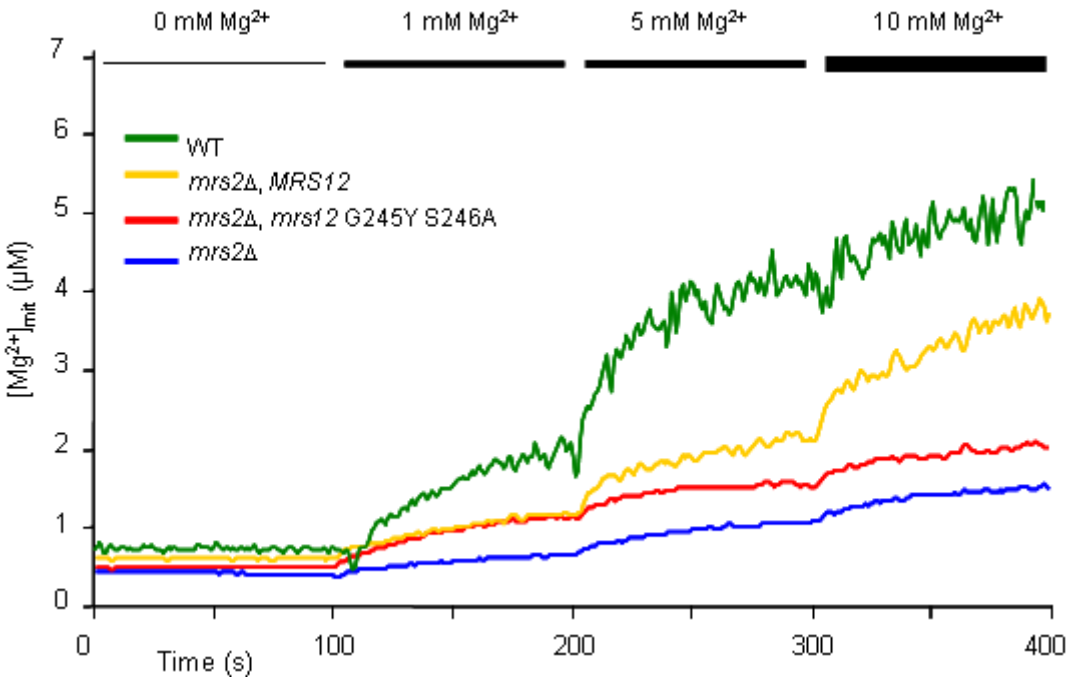

Figure 17: Mg^{2+}-uptake into mitochondria by Mrs12p and Mrs12p G245Y S246A. Mitochondria were isolated from DBY747 (wild-type) and DBY7474 *mrs2*Δ and loaded with mag-fura2. Samples were measured with a spectroflourometer at excitation wavelengths 340 and 380 nm and emission wavelength 509 nm. External $[Mg^{2+}]$ was increased to final concentrations of 1, 5 and 10 mM as described in materials and methods.

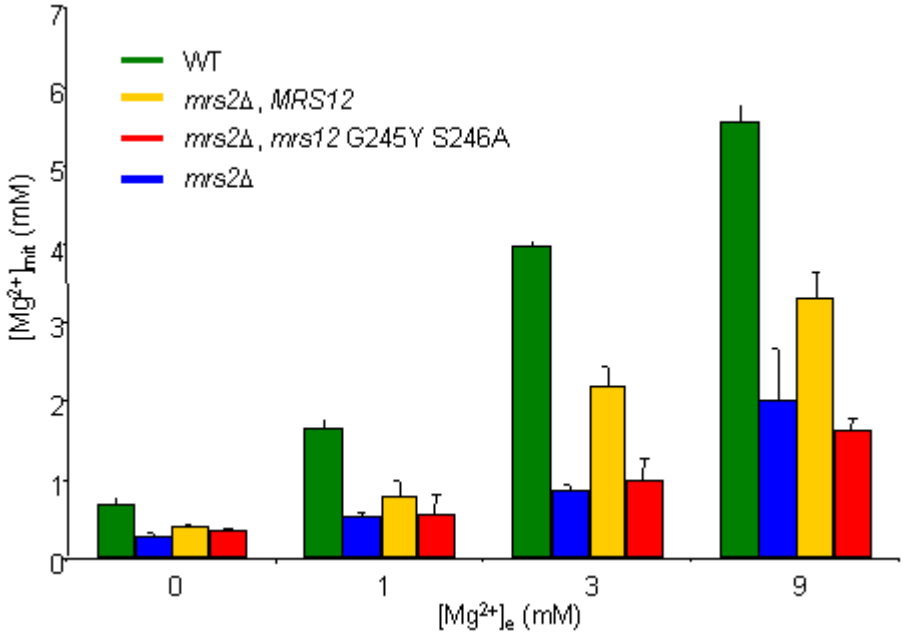

Figure 18: Quantification of Mg^{2+}-uptake into mitochondria by Mrs12p and Mrs12p G245Y S246A. Preparation of samples was carried out as described in Figure 16 and $[Mg^{2+}]_{int}$ values were calculated as described in materials and methods.

5 Discussion

Iron uptake into mitochondria is proposed to be accomplished by the two mitochondrial carrier proteins Mrs3/4p. However, it has been suggested that these two proteins do not represent the sole system for iron uptake, as the *mrs3/4*Δ phenotype is only observed under iron limiting conditions (Muhlenhoff, Stadler et al. 2003). If iron supply in the cytoplasm is sufficient, iron seems to enter the mitochondrion by another route. When searching for a possible candidate for iron transport under normal iron concentrations, the *MRS12* gene, which codes for the mitochondrial pyrimidine nucleotide transporter (Marobbio, Di Noia et al. 2006), was surprisingly found to act as multi-copy suppressor of the *mrs3/4*Δ phenotype. To our knowledge, no connection between pyrimidine transport and iron uptake into mitochondria has been observed to date.

In this work, an attempt to characterize Mrs12p function in relation to mitochondrial iron metabolism and general metal uptake was performed, which support Mrs12p's role in divalent metal transport.

In a first experiment, we wanted to investigate whether there is a connection between *MRS12* expression and cellular iron homeostasis. In order to study this, we performed a *FET3*-GFP assay. *FET3* is a ferro-oxidoreductase at the yeast cell surface, which imports iron when it is present in low concentrations (Askwith, Eide et al. 1994). Upon mitochondrial iron depletion, *FET3* expression is induced by the iron sensing transcription regulator Aft1p and it is also induced in *mrs3/4*Δ cells. In the assay, the triple mutant showed higher expression of the ferro-oxidoreductase than the *mrs3/4*Δ mutant did, which implies that *mrs3/4/12*Δ cells suffer from higher iron deprivation than *mrs3/4*Δ cells. For *mrs12*Δ cells, no significant up-regulation of *FET3* was detected. Given the fact that Mrs3/4p are still present in these cells, they probably contain enough iron in their mitochondria and so there is no considerable shortage of the metal to induce *FET3*-expression, especially when the cells are grown in iron-rich media. In this assay, a link between *MRS12* and *FET3* expression (and therefore cellular iron homeostasis) can only be indirectly observed by comparing *mrs3/4*Δ and *mrs3/4/12*Δ cells. Therefore, we performed genome wide expression profiling of *mrs12*Δ and *mrs3/4/12*Δ cells to look for other genes involved in iron transport, which might be up-regulated in the mutants.

Genome wide expression profiling of *mrs12*Δ cells revealed that the two siderophore-iron transporters *FIT2* and *FIT3*, which belong to the iron regulon and are under the control of Aft1p, were induced (Wiesenberger, unpublished results). This result represents a link between *MRS12* and cellular iron homeostasis. *mrs12*Δ cells seem to need elevated

concentrations of iron in their cytoplasm compared to wild-type cells to provide the mitochondria with normal iron dosages. Why are *FIT2/3*, but no other genes of the iron regulon induced in *mrs12*Δ cells? An explanation could be that it is not necessary for the cell to also induce expression of other iron-related proteins because, in the presence of the high-affinity iron transporters Mrs3/4p, higher cytosolic iron concentrations automatically lead to higher mitochondrial iron content and the additional amount of iron taken up by *FIT2/3* into the cytoplasm is sufficient to compensate for loss of iron transported into mitochondria by Mrs12p.

Genome wide expression profiling of *mrs3/4/12*Δ cells showed up-regulation of several genes belonging to the iron regulon. This finding was to be expected, as *mrs3/4*Δ cells already show induction of the iron regulon (Muhlenhoff, Stadler et al. 2003). Upon mitochondrial iron deprivation due to the absence of Mrs3/4p, mitochondrial iron-sulfur clusters cause activation of the iron-sensing transcription factor Aft1p, which in turn induces genes essential for iron uptake and iron transport into the cell to compensate for the diminished mitochondrial iron content (Rutherford, Ojeda et al. 2005). In the *mrs3/4/12*Δ mutant, induction of several genes of the iron regulon was observed, providing evidence for severe mitochondrial iron deprivation.

According to the findings of the microarray and the *FET3*-Assay, Mrs12p can be linked to mitochondrial iron uptake and could be involved in low-affinity iron transport. It should be considered that, if Mrs3p, Mrs4p and Mrs12p were the only transporters delivering iron into mitochondria, absence of all three proteins would be lethal for the cell, as iron is needed for carrying out Fe-S biogenesis, which is an essential mitochondrial process (Lill, Diekert et al. 1999). However, the *mrs3/4/12*Δ mutant is still viable, which would mean that iron uptake into mitochondria is, although reduced to a great extent, not totally abolished and that other low-affinity iron transporters are probably present.

In order to study the connection between pyrimidine transport and suppression of the *mrs3/4*Δ phenotype a mutant in contact point II, a proposed substrate binding site of mitochondrial carrier proteins (Robinson and Kunji 2006), was created. The amino acids glycine 245 and serine 246 were changed into tyrosine and alanine by *in vitro* mutagenesis. The mutated protein was stably expressed, but did not show complementation of the *mrs12*Δ mutation and was not able to transport pyrimidine nucleotides into mitochondria, demonstrating that mutations at this site affect the function, but not the stability of the protein. In mitochondrial carrier proteins, contact point II is essential for distinguishing between different substrates forming a hydrophobic pocket for substrate binding (Robinson and Kunji 2006). We assume

that by changing glycine and serine into tyrosine and alanine this hydrophobic pocket is destroyed and substrate binding is not properly achieved. Furthermore, suppression of the *mrs3/4*Δ phenotype by mutated *mrs12* G2245Y S246A is not observed in the mutant anymore. Also, iron transport into submitochondrial particles was studied in *mrs3/4*Δ and *mrs3/4*Δ SMPs overexpressing *MRS12*, which showed that, upon addition of pyrimidine nucleotides, iron is readily taken up into SMPs overexpressing *MRS12*, but uptake was significantly reduced in the mutant. Thus, we suggest that Mrs12p might mediate iron uptake into yeast mitochondria via pyrimidine transport. Pyrimidine uptake into mitochondria is essential for suppression of the *mrs3/4*Δ phenotype, and it is probable that iron is co-transported with pyrimidine nucleotides.

Assuming this transport mechanism, Mrs12p might transport other divalent metals in a similar manner, especially as it had already been shown that overexpression of *MRS12* suppresses the *mrs2*Δ phenotype (Van Dyck, Jank et al. 1995). The phenotype is due to the absence of the main mitochondrial Mg^{2+} transporter Mrs2p (Kolisek, Zsurka et al. 2003), indicating that Mrs12p might be involved in Mg^{2+} uptake by a similar mechanism as in Fe^{2+} uptake. To test this, growth tests of *mrs2*Δ cells overexpressing *MRS12* or the mutant were performed, showing that overexpression of *MRS12* suppresses the *mrs2*Δ phenotype, whereas overexpression of the mutant does not. Mg^{2+}-Uptake studies into isolated mitochondria using the Mg^{2+} chelator mag-fura 2 resulted in another observation confirming Mrs12p's involvement in mitochondrial Mg^{2+}-acquisition. Here, Mg^{2+}-uptake was increased in *mrs2*Δ mitochondria when *MRS12* was overexpressed, but not when the mutant was overexpressed. However, upon addition of pyrimidines and Mg^{2+} to mitochondria, pyrimidines bind Mg^{2+}, which unfortunately interferes with the experimental set-up. Therefore, the influence of pyrimidine transport on Mg^{2+} uptake by Mrs12p could not be properly studied, but it presents, together with the finding that the mutant mediates much lower Mg^{2+} uptake than wild-type Mrs12p, an indication that pyrimidines have to be transported by Mrs12p in order for divalent metals to be taken up by mitochondria. Thus, our findings indicate that Mrs12p is likely to have a function as low-affinity divalent metal transporter by coupling pyrimidine uptake to metal transport.

How and why might iron be transported by pyrimidine nucleotides via Mrs12p in the mitochondrion? A possibility is that iron is complexed to the phosphate moieties of pyrimidine nucleotides in a similar way as Mg^{2+} is proposed to interact with ATP in the Mg^{2+}-ATP/P_i carrier Sal1p. As anion transport into mitochondria is opposed by the electrochemical

gradient, coupling their transport to cations provides a way of driving them into the mitochondrion against the electrochemical gradient, which might be the case for Sal1p. In Sal1p, the phosphate-coordinated magnesium cation interacts with the amino acid glutamate E318 at contact point I, which contains the amino acids lysine K314, glutamate E318 and lysine K322. A water molecule may be involved in the coordination of the Mg^{2+} ion. In Mrs12p, contact point I includes the amino acids glycine G145, alanine A149 and asparagine N153, alanine A149 would correspond to glutamate E318 in Sal1p (Robinson and Kunji 2006). Glutamate is a negatively charged amino acid, which can coordinate Mg^{2+}, whereas alanine is a non-polar amino acid and does not coordinate Mg^{2+}. Also, Mrs12p's affinity towards iron is higher than towards magnesium, as iron uptake into SMPs is not inhibited upon addition of aequimolar concentrations of Mg^{2+} (Froschauer, unpublished results). *In vivo*, Mg^{2+} concentrations exceed Fe^{2+} concentrations by a factor of about 500, and it is unlikely that Fe^{2+} would be transported into the mitochondrion if divalent metal transport by Mrs12p was completely unspecific. However, different affinities of Mrs12p towards Fe^{2+} and Mg^{2+} would provide an explanation why Fe^{2+} is transported. The question of how iron might coordinate to amino acids and substrate, however, is not clear. If there is a role of Mrs12p contact point I in coordinating iron, comparative modeling and random mutagenesis studies of amino acids residues might provide a clue how binding and transport of iron is established.

Given that Mrs12p can mediate iron and magnesium uptake, transport of other relevant divalent metals like Zn^{2+}, Cu^{2+} and Mn^{2+} is likely to occur as well. Zn^{2+} is needed in mitochondria as cofactor for several enzymes (Zim17p, Mdj1p) and in Zn-metalloenzymes, which are, i.e., involved in alcohol oxidation or leucine biosynthesis (Adh3p, Adh4p, Leu9p) or act as metalloproteases. Copper is required for the assembly of cytochrome c oxidase and superoxide dismutase. Mitochondrial Mn^{2+}'s only known function is as a cofactor in Mn-superoxide dismutase, which is important in the protection against oxidative damage (Pierrel, Cobine et al. 2007). So far, no mitochondrial transport proteins have been identified for these transition metals. However, studies with SMPs demonstrate that Cu^{2+} and Zn^{2+} uptake are elevated in SMPs deriving from cells overexpressing *MRS12* when compared to wild-type SMPs, but not from cells overexpressing the mutant. Interestingly, if the pH inside SMPs is lowered, Fe^{2+} uptake into *mrs3/4*Δ SMPs carrying Mrs12p decreases (Froschauer, unpublished results). According to these data, Mrs12p seems to be able to mediate uptake of other transition metals besides iron as well and therefore could function as low-affinity divalent metal transporter in mitochondria. As mentioned above, coupling anion transport across the inner mitochondrial membrane to cations represents a way of driving them into the

mitochondrion against the electrochemical gradient. The transport of pyrimidines and cations might depend on the electrochemical gradient, as uptake decreases when the pH inside SMPs is lowered.

Considering that mitochondria possess several transporters belonging to the mitochondrial carrier family, which transport a variety of substrates from nucleotides to amino acids across the inner mitochondrial membrane, the pyrimidine transporter Mrs12p might not be the only transporter involved in metal uptake. Studies have shown that the mitochondrial GTP/GDP carrier protein Ggc1p plays a role in mitochondrial iron metabolism, as absence of Ggc1p leads to high cellular iron uptake and iron accumulation in the mitochondrial matrix (Lesuisse, Lyver et al. 2004). Normal iron regulation is restored when a human nucleoside diphosphate kinase, which converts ATP into GTP, is targeted to the matrix of *ggc1*Δ mutants (Gordon, Lyver et al. 2006). However, there is no link to mitochondrial iron uptake in this study. According to the authors, mitochondrial iron metabolism is affected by GTP/GDP levels in the mitochondrial matrix and absence of GTP leads to accumulation of iron. Also, a recent study shows that GTP is required for iron-sulfur cluster biogenesis in mitochondria (Amutha, Gordon et al. 2008), which might be an explanation for iron accumulation in the mutant. Given that our findings point to a role of the pyrimidine transporter Mrs12p in iron uptake, it can still be speculated that the purine Gcg1p transporter might mediate iron uptake via purine transport, but suppression experiments in *mrs3/4*Δ strains overexpressing *GCG1* have to be performed in order to study this in more detail.

It should also be mentioned that in an attempt to find further suppressors of the *mrs3/4*Δ iron phenotype, a *mrs3/4*Δ mutant was transformed with a library obtained from a *mrs3/4/12*Δ strain, but only very weak suppressors (i.e. *ORC1*, which codes for the mitochondrial ornithine transporter (Fiermonte, Dolce *et al*. 2003)) compared to *MRS12* were found (Wiesenberger, Binder, personal communication). This suggests that only *MRS12* can suppress the iron phenotype of *mrs3/4*Δ mutants under the conditions of the screen and that there might be no other transporter involved in iron transport.

What is the physiological relevance of our findings? A speculative scenario is that yeast mitochondria comprise a general unspecific cation uptake system coupled to anion transport, which has been observed for Mrs12p or Sal1p and might also be of relevance for other mitochondrial carriers, and a specific cation uptake system, which contains high-affinity iron transporters Mrs3/4p, the Mg^{2+} channel Mrs2p and other not yet identified proteins. Selectivity is not required in the case of the general uptake system, as it only supplies the mitochondrion with basal metal concentrations. When a specific ion is needed inside the

matrix, high-affinity transporters mediate selective cation uptake and ensure adequate metal ion supply. This system would provide yeast mitochondria the ability to adapt to metal ion availability and to regulate uptake and distribution of metal ions accordingly.

6 Appendix

6.1 Plasmid Maps

pMH1

Plasmid: pMH1 **Date:** 03/03/08

Backbone: pCM189 **Size:** 9,600 kb

Markers: Amp^r, *URA3*

Host Strain: DH10B

References: MH book 779, p005

Stock: *E. coli* box (freezer cultures)

Construction: pAS14 (*MRS12*-HA in pCM189) was cleaved with BamHI, treated with Cip and ligated to a 1.2 kb BamHI fragment containing the *mrs12* G245Y, S246A gene.

Comment: No backup clone (clone contains additional mutation)

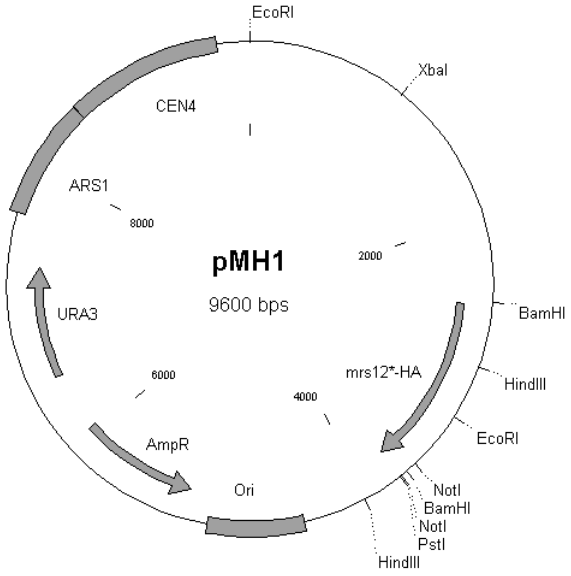

pMH2

Plasmid: pMH2 **Date:** 05/03/08

Backbone: pCM189 **Size:** 9,489 kb

Markers: Amp^r, *URA3*

Host Strain: DH10B

References: MH book 779, p007

Stock: *E. coli* box (freezer cultures)

Construction: pMH1 (*mrs12* G245Y, S246A-HA in pCM189) was cleaved with NotI to cut out HA-tag and religated

Comment: 1 backup clone

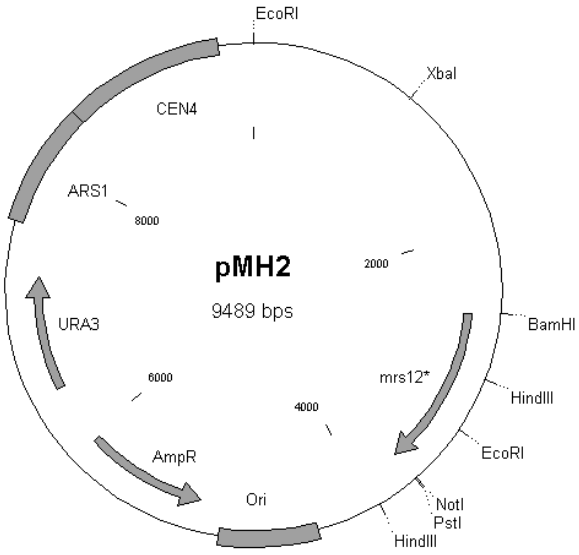

pMH3

Plasmid: pMH3 **Date:** 10/03/08

Backbone: YCpLac33 **Size:** 7,733 kb

Markers: Amp^r, *URA3*

Host Strain: DH10B

References: MH book 779, p010

Stock: *E. coli* box (freezer cultures)

Construction: pOLU2 (*MRS12* in YCplac33) was cleaved with HindIII, treated with Cip and the 6.7 kb fragment was ligated to the 1.2 kb HindIII fragment from pAS12 (*MRS12* in pCM189).

Comment: 1 backup clone

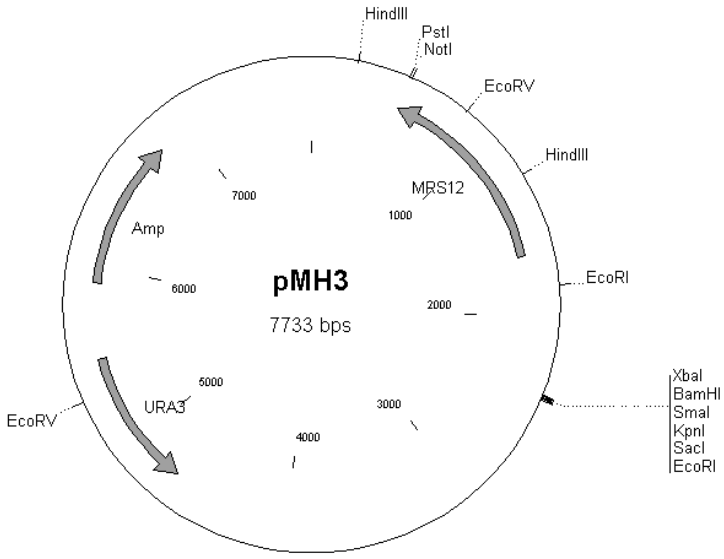

pMH4

Plasmid: pMH4 **Date:** 10/03/08

Backbone: YCpLac33 **Size:** 7,844 kb

Markers: Amp^r, *URA3*

Host Strain: DH10B

References: MH book 779, p010

Stock: *E. coli* box (freezer cultures)

Construction: pOLU2 (*MRS12* in YCplac33) was cleaved with HindIII, treated with Cip and the 6.7 kb fragment was ligated to the 1.2 kb HindIII fragment from pMH1 (*mrs12* G245Y, S246A -HA in pCM189).

Comment: 1 backup clone

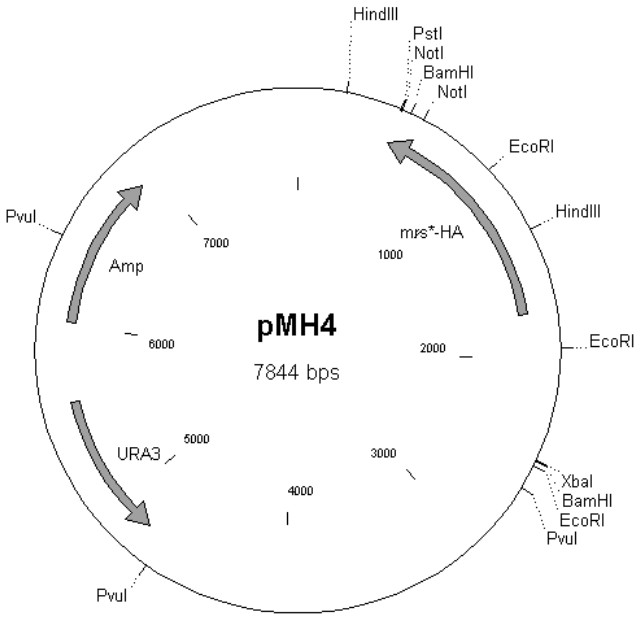

pMH5

Plasmid: pMH5 **Date:** 10/03/08

Backbone: YCpLac33 **Size:** 7,733 kb

Markers: Amp^r, *URA3*

Host Strain: DH10B

References: MH book 779, p010

Stock: *E. coli* box (freezer cultures)

Construction: pOLU2 (*MRS12* in YCplac33) was cleaved with HindIII, treated with Cip and the 6.7 kb fragment was ligated to the 1.2 kb HindIII fragment from pMH2 (*mrs12* G245Y, S246A in pCM189).

Comment: 1 backup clone

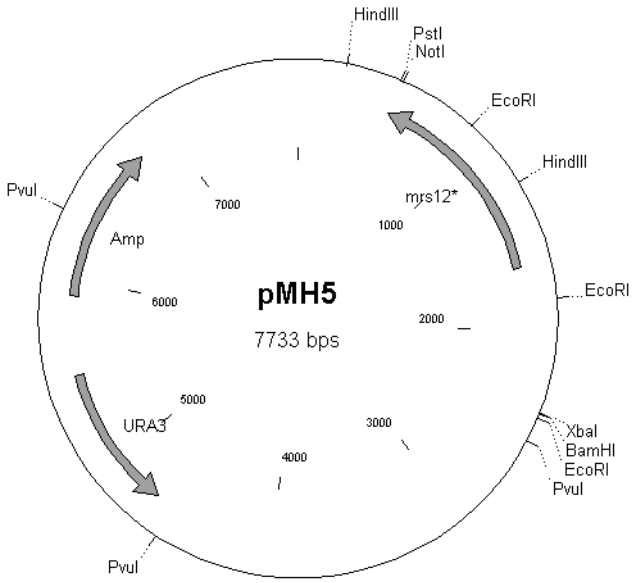

pAS12

Plasmid: pAS12

Backbone: pCM189 **Size:** 9,489 kb

Markers: Amp^r, *URA3*

Host Strain: DH10B

References: MH book 778, 779

Stock: *E. coli* box (freezer cultures)

Construction: *MRS12* was cleaved with *Bam*HI/*Pst*I from pAS17 and the 1,2 kb fragment containing the *MRS12* ORF was ligated into pCM189 cut with the same enzymes. The resulting plasmid was called pAS 12

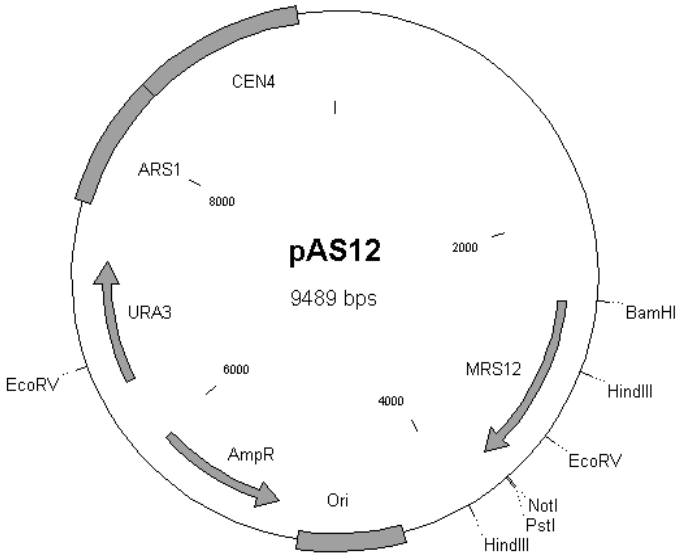

pAS14

Plasmid: pAS14

Backbone: pCM189 **Size:** 9,600 kb

Markers: Amp^r, *URA3*

Host Strain: DH10B

References: MH book 778, 779

Stock: *E. coli* box (freezer cultures)

Construction: The HA-tag was cut out with *Not*I from YEp351-HA and inserted in frame into *Not*I cleaved pAS12 resulting in an in frame fusion of the HA tag to the *MRS12* ORF (by Axel Struß).

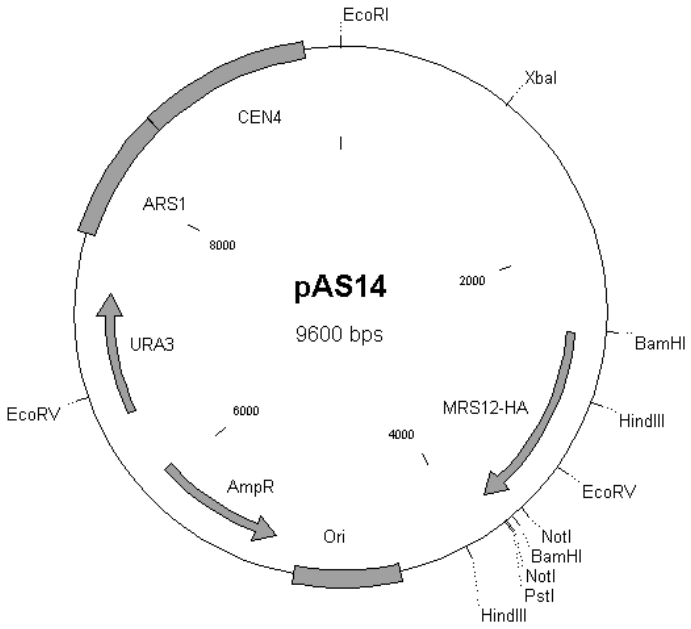

pOLU2

Plasmid: pOLU2

Backbone: YCpLac33 **Size:** 8,834 kb

Markers: Amp^r, *URA3*

Host Strain: DH10B

References: MH book 779

Stock: *E. coli* box (freezer cultures)

Construction: A 3.2kb *Xba*I fragment from *MRS12*.Yep351 (Gerlinde) was cloned into *Xba*I site of YCplac33.

Comment: "Anti sense" Orientation with respect to the polylinker (*Hind*III-*Eco*RI)

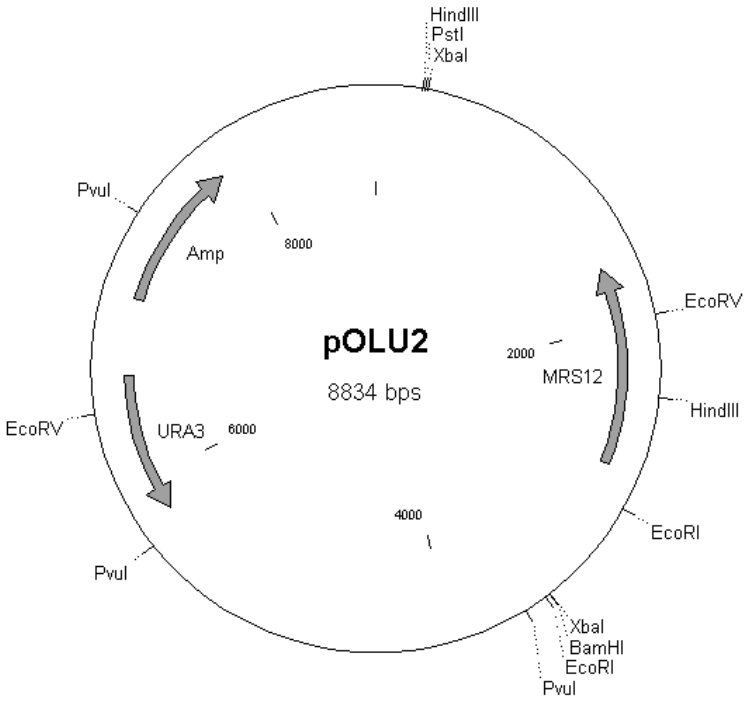

7 References

Alberts, B., A. Johnson, et al. (2007). Molecular Biology of the Cell - Fifth Edition, Garland Science.

Amutha, B., D. M. Gordon, et al. (2008). "GTP is required for iron-sulfur cluster biogenesis in mitochondria." J Biol Chem **283**(3): 1362-71.

Andrews, N. C. (2000). "Iron homeostasis: insights from genetics and animal models." Nat Rev Genet **1**(3): 208-17.

Andrews, N. C. (2002). "Metal transporters and disease." Curr Opin Chem Biol **6**(2): 181-6.

Askwith, C., D. Eide, et al. (1994). "The FET3 gene of S. cerevisiae encodes a multicopper oxidase required for ferrous iron uptake." Cell **76**(2): 403-10.

Bui, D. M., J. Gregan, et al. (1999). "The bacterial magnesium transporter CorA can functionally substitute for its putative homologue Mrs2p in the yeast inner mitochondrial membrane." J Biol Chem **274**(29): 20438-43.

Casey, J. L., M. W. Hentze, et al. (1988). "Iron-responsive elements: regulatory RNA sequences that control mRNA levels and translation." Science **240**(4854): 924-8.

De Domenico, I., D. McVey Ward, et al. (2008). "Regulation of iron acquisition and storage: consequences for iron-linked disorders." Nat Rev Mol Cell Biol **9**(1): 72-81.

Ernst, J. F., R. L. Bennett, et al. (1978). "Constitutive expression of the iron-enterochelin and ferrichrome uptake systems in a mutant strain of Salmonella typhimurium." J Bacteriol **135**(3): 928-34.

Fiermonte, G., V. Dolce, et al. (2003). "The mitochondrial ornithine transporter. Bacterial expression, reconstitution, functional characterization, and tissue distribution of two human isoforms." J Biol Chem **278**(35): 32778-83.

Foury, F. and T. Roganti (2002). "Deletion of the mitochondrial carrier genes MRS3 and MRS4 suppresses mitochondrial iron accumulation in a yeast frataxin-deficient strain." J Biol Chem **277**(27): 24475-83.

Georgatsou, E. and D. Alexandraki (1994). "Two distinctly regulated genes are required for ferric reduction, the first step of iron uptake in Saccharomyces cerevisiae." Mol Cell Biol **14**(5): 3065-73.

Gordon, D. M., E. R. Lyver, et al. (2006). "GTP in the mitochondrial matrix plays a crucial role in organellar iron homoeostasis." Biochem J **400**(1): 163-8.

Grynkiewicz, G., M. Poenie, et al. (1985). "A new generation of Ca2+ indicators with greatly improved fluorescence properties." J Biol Chem **260**(6): 3440-50.

Gunshin, H., B. Mackenzie, et al. (1997). "Cloning and characterization of a mammalian proton-coupled metal-ion transporter." Nature **388**(6641): 482-8.

Hanahan, D. (1983). "Studies on transformation of Escherichia coli with plasmids." J Mol Biol **166**(4): 557-80.

Harris, Z. L., A. P. Durley, et al. (1999). "Targeted gene disruption reveals an essential role for ceruloplasmin in cellular iron efflux." Proc Natl Acad Sci U S A **96**(19): 10812-7.

Harrison, P. M. and P. Arosio (1996). "The ferritins: molecular properties, iron storage function and cellular regulation." Biochim Biophys Acta **1275**(3): 161-203.

Hentze, M. W. and L. C. Kuhn (1996). "Molecular control of vertebrate iron metabolism: mRNA-based regulatory circuits operated by iron, nitric oxide, and oxidative stress." Proc Natl Acad Sci U S A **93**(16): 8175-82.

Hentze, M. W., M. U. Muckenthaler, et al. (2004). "Balancing acts: molecular control of mammalian iron metabolism." Cell **117**(3): 285-97.

Kaplan, J., D. McVey Ward, et al. (2006). "Iron-dependent metabolic remodeling in S. cerevisiae." Biochim Biophys Acta **1763**(7): 646-51.

Knight, S. A., N. B. Sepuri, et al. (1998). "Mt-Hsp70 homolog, Ssc2p, required for maturation of yeast frataxin and mitochondrial iron homeostasis." J Biol Chem **273**(29): 18389-93.
Kolisek, M., G. Zsurka, et al. (2003). "Mrs2p is an essential component of the major electrophoretic Mg2+ influx system in mitochondria." Embo J **22**(6): 1235-44.
Kunji, E. R. and A. J. Robinson (2006). "The conserved substrate binding site of mitochondrial carriers." Biochim Biophys Acta **1757**(9-10): 1237-48.
Lange, H., G. Kispal, et al. (1999). "Mechanism of iron transport to the site of heme synthesis inside yeast mitochondria." J Biol Chem **274**(27): 18989-96.
Lebron, J. A., A. P. West, Jr., et al. (1999). "The hemochromatosis protein HFE competes with transferrin for binding to the transferrin receptor." J Mol Biol **294**(1): 239-45.
Lesuisse, E., E. R. Lyver, et al. (2004). "Role of YHM1, encoding a mitochondrial carrier protein, in iron distribution of yeast." Biochem J **378**(Pt 2): 599-607.
Li, J., M. Kogan, et al. (1999). "Yeast mitochondrial protein, Nfs1p, coordinately regulates iron-sulfur cluster proteins, cellular iron uptake, and iron distribution." J Biol Chem **274**(46): 33025-34.
Li, L. and J. Kaplan (2004). "A mitochondrial-vacuolar signaling pathway in yeast that affects iron and copper metabolism." J Biol Chem **279**(32): 33653-61.
Lill, R., K. Diekert, et al. (1999). "The essential role of mitochondria in the biogenesis of cellular iron-sulfur proteins." Biol Chem **380**(10): 1157-66.
Lok, C. N. and P. Ponka (1999). "Identification of a hypoxia response element in the transferrin receptor gene." J Biol Chem **274**(34): 24147-52.
Marobbio, C. M., M. A. Di Noia, et al. (2006). "Identification of a mitochondrial transporter for pyrimidine nucleotides in Saccharomyces cerevisiae: bacterial expression, reconstitution and functional characterization." Biochem J **393**(Pt 2): 441-6.
Masse, E. and M. Arguin (2005). "Ironing out the problem: new mechanisms of iron homeostasis." Trends Biochem Sci **30**(8): 462-8.
McKie, A. T., P. Marciani, et al. (2000). "A novel duodenal iron-regulated transporter, IREG1, implicated in the basolateral transfer of iron to the circulation." Mol Cell **5**(2): 299-309.
Muhlenhoff, U., J. A. Stadler, et al. (2003). "A specific role of the yeast mitochondrial carriers MRS3/4p in mitochondrial iron acquisition under iron-limiting conditions." J Biol Chem **278**(42): 40612-20.
Nemeth, E., M. S. Tuttle, et al. (2004). "Hepcidin regulates cellular iron efflux by binding to ferroportin and inducing its internalization." Science **306**(5704): 2090-3.
Palmieri, F., G. Agrimi, et al. (2006). "Identification of mitochondrial carriers in Saccharomyces cerevisiae by transport assay of reconstituted recombinant proteins." Biochim Biophys Acta **1757**(9-10): 1249-62.
Pandolfo, M. (2008). "Friedreich ataxia." Arch Neurol **65**(10): 1296-303.
Papanikolaou, G. and K. Pantopoulos (2005). "Iron metabolism and toxicity." Toxicol Appl Pharmacol **202**(2): 199-211.
Pebay-Peyroula, E., C. Dahout-Gonzalez, et al. (2003). "Structure of mitochondrial ADP/ATP carrier in complex with carboxyatractyloside." Nature **426**(6962): 39-44.
Pierrel, F., P. A. Cobine, et al. (2007). "Metal Ion availability in mitochondria." Biometals **20**(3-4): 675-82.
Ponka, P., C. Beaumont, et al. (1998). "Function and regulation of transferrin and ferritin." Semin Hematol **35**(1): 35-54.
Puig, S., E. Askeland, et al. (2005). "Coordinated remodeling of cellular metabolism during iron deficiency through targeted mRNA degradation." Cell **120**(1): 99-110.
Robinson, A. J. and E. R. Kunji (2006). "Mitochondrial carriers in the cytoplasmic state have a common substrate binding site." Proc Natl Acad Sci U S A **103**(8): 2617-22.

Rutherford, J. C., S. Jaron, et al. (2001). "A second iron-regulatory system in yeast independent of Aft1p." Proc Natl Acad Sci U S A **98**(25): 14322-7.
Rutherford, J. C., S. Jaron, et al. (2003). "Aft1p and Aft2p mediate iron-responsive gene expression in yeast through related promoter elements." J Biol Chem **278**(30): 27636-43.
Rutherford, J. C., L. Ojeda, et al. (2005). "Activation of the iron regulon by the yeast Aft1/Aft2 transcription factors depends on mitochondrial but not cytosolic iron-sulfur protein biogenesis." J Biol Chem **280**(11): 10135-40.
Schaible, U. E. and S. H. Kaufmann (2004). "Iron and microbial infection." Nat Rev Microbiol **2**(12): 946-53.
Schilke, B., C. Voisine, et al. (1999). "Evidence for a conserved system for iron metabolism in the mitochondria of Saccharomyces cerevisiae." Proc Natl Acad Sci U S A **96**(18): 10206-11.
Shakoury-Elizeh, M., J. Tiedeman, et al. (2004). "Transcriptional remodeling in response to iron deprivation in Saccharomyces cerevisiae." Mol Biol Cell **15**(3): 1233-43.
Van Dyck, E., B. Jank, et al. (1995). "Overexpression of a novel member of the mitochondrial carrier family rescues defects in both DNA and RNA metabolism in yeast mitochondria." Mol Gen Genet **246**(4): 426-36.
Van Ho, A., D. M. Ward, et al. (2002). "Transition metal transport in yeast." Annu Rev Microbiol **56**: 237-61.
Vulpe, C. D., Y. M. Kuo, et al. (1999). "Hephaestin, a ceruloplasmin homologue implicated in intestinal iron transport, is defective in the sla mouse." Nat Genet **21**(2): 195-9.
Waldherr, M., A. Ragnini, et al. (1993). "A multitude of suppressors of group II intron-splicing defects in yeast." Curr Genet **24**(4): 301-6.
Wiesenberger, G., T. A. Link, et al. (1991). "MRS3 and MRS4, two suppressors of mtRNA splicing defects in yeast, are new members of the mitochondrial carrier family." J Mol Biol **217**(1): 23-37.
Yamaguchi-Iwai, Y., A. Dancis, et al. (1995). "AFT1: a mediator of iron regulated transcriptional control in Saccharomyces cerevisiae." Embo J **14**(6): 1231-9.
Yamaguchi-Iwai, Y., R. Ueta, et al. (2002). "Subcellular localization of Aft1 transcription factor responds to iron status in Saccharomyces cerevisiae." J Biol Chem **277**(21): 18914-8.

8 Acknowledgements

Reaching the final stage of my diploma study, I would like to thank my family for supporting me during the last few years. My parents and my grandparents enabled me to follow my interests and put plenty of efforts in my study, which I would not have been able to do without their continued assistance and financial aid. Special thanks go to my mother and my sister, who have often been patient listeners of my struggles and problems and were always there to encourage me and provide me with their advice. I'd also like to thank my friends, those I've known since school, those who are or have been living at Vienna, and those I've met during my studies abroad. All of you are special people whose company I am always glad to enjoy.

I am also thankful for the perfect supervision provided by Gerlinde Wiesenberger. I have learned a lot regarding all aspects of scientific work by her guidance and her detailed explanations and feel really grateful for her commitment in all phases of my work.

Thanks also to Elisabeth Froschauer and Jochen Stadler for teaching me new lab techniques and for sharing their work outcomes with me, and to Prof. Rudolf Schweyen for supporting and discussing my work. Finally, thanks to all past and present members of the Schweyen Group, who always helped me whenever I needed something or when I had questions in the lab. I really enjoyed our lunch break discussions and lab events and I am glad to have been working with you all.

9 Curriculum Vitae

Personal Details

Name:	Melanie Rosalia Hassler
Address:	Weidenweg 6, 9063 Maria Saal (home)
	Johannagasse 19/3/14, 1050 Vienna (term time)
e-mail:	melanie.hassler1@gmx.at
Date of birth:	16. November 1983, St. Veit an der Glan
Nationality:	Austrian
Marital status:	single

Education and Qualifications

1990 – 1994	Elementary School Maria Saal
1994 – 2002	Europagymnasium Klagenfurt
June 2002	Matura (A-Levels) with distinction
since 2002	Study of Chemistry at the University of Vienna
October 2005	First diploma examination in Chemistry (passed with highest honours) and following specialisation in biochemistry, food chemistry and molecular biology
Jan-Dec 2008	Diploma Thesis at Department of Genetics (thesis project: "The mitochondrial pyrimidine transporter Mrs12p mediates iron uptake into yeast mitochondria")

International Experience

March -June 2006	Erasmus-term at the University of Warwick, Coventry, UK, Department of Chemistry (research project: "MhpC Lactonisation and Hydroxamic Acid Production")
Oct - Dec 2007	IAESTE Internship at the Universidade Nova de Lisboa, Lisbon, Portugal, Department of Chemistry (research project: "Purification and Characterisation of Denitrifying Enzymes of *Pseudomonas nautica*")

Scholarships

WS03, WS07	Scholarships for outstanding study performance